Silicon strip detector upgrade for AMS-02 and AI/ML application

Dexing Miao(缪德星)
miaodx@ihep.ac.cn

30/09/2025, CCNU

中国科学院高能物理研究所
Institute of High Energy Physics Chinese Academy of Sciences

Self Introduction

Education

- 2017 Sep. – 2021 Jun.
  - B.S.in Materials Science, 武汉理工大学
  - B.S. in Computer Science and Technology, 武汉大学
- 2021 Sep. – 2026 Jun.
  - Ph.D. candidate, IHEP
  - 2023 Sep. – 2024 Sep, CSC found, INFN and CERN

Research

- Silicon strip detector upgrade for AMS-02: Detector construction, Telescope development, E-test, Beam test, Detector performance study
- ML algorithm development

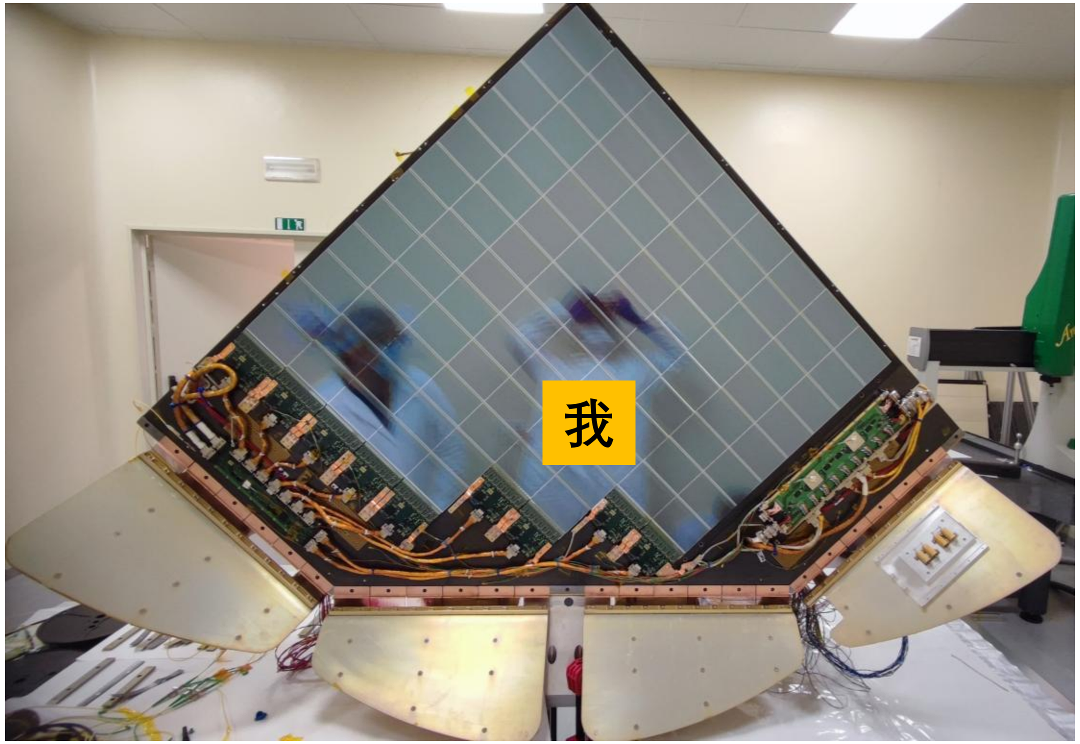

AMS on the Space Station

Provides precision, long-duration measurements of charged cosmic rays to study the Origin of the Cosmos, the physics of Dark Matter and Antimatter

Charged cosmic rays have mass.
They are absorbed by the
100 km of Earth's atmosphere (10m of water).
The properties ($\pm Z$, P) of charged cosmic rays cannot be studied on the ground.

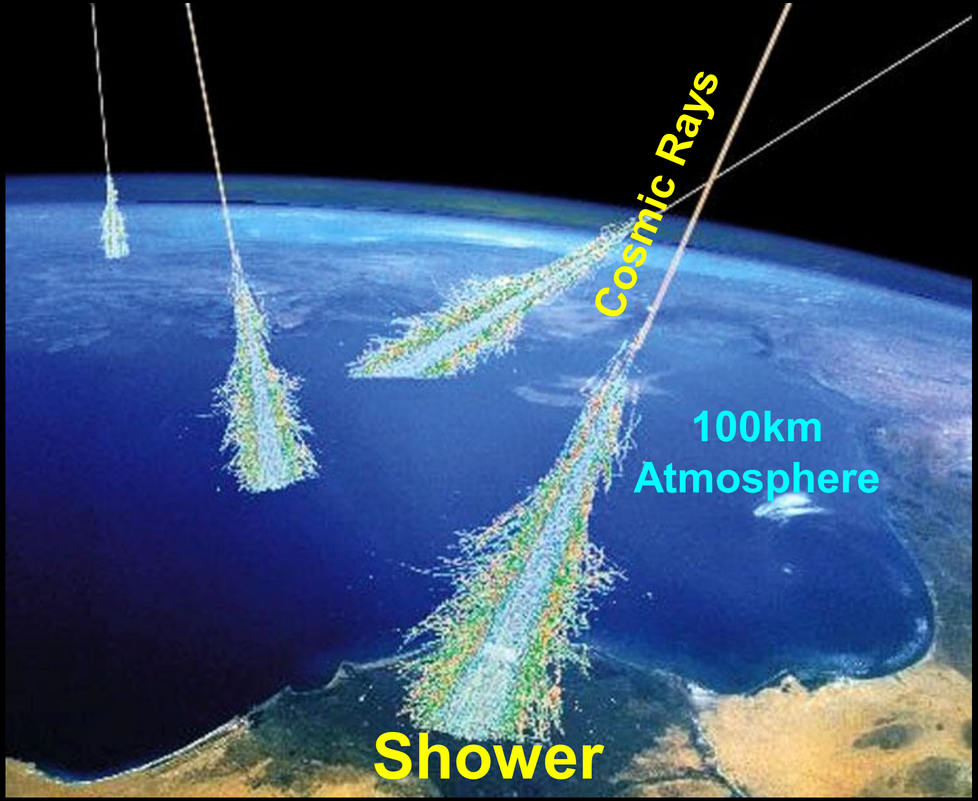

To measure cosmic ray charge and momentum requires a magnetic spectrometer in space

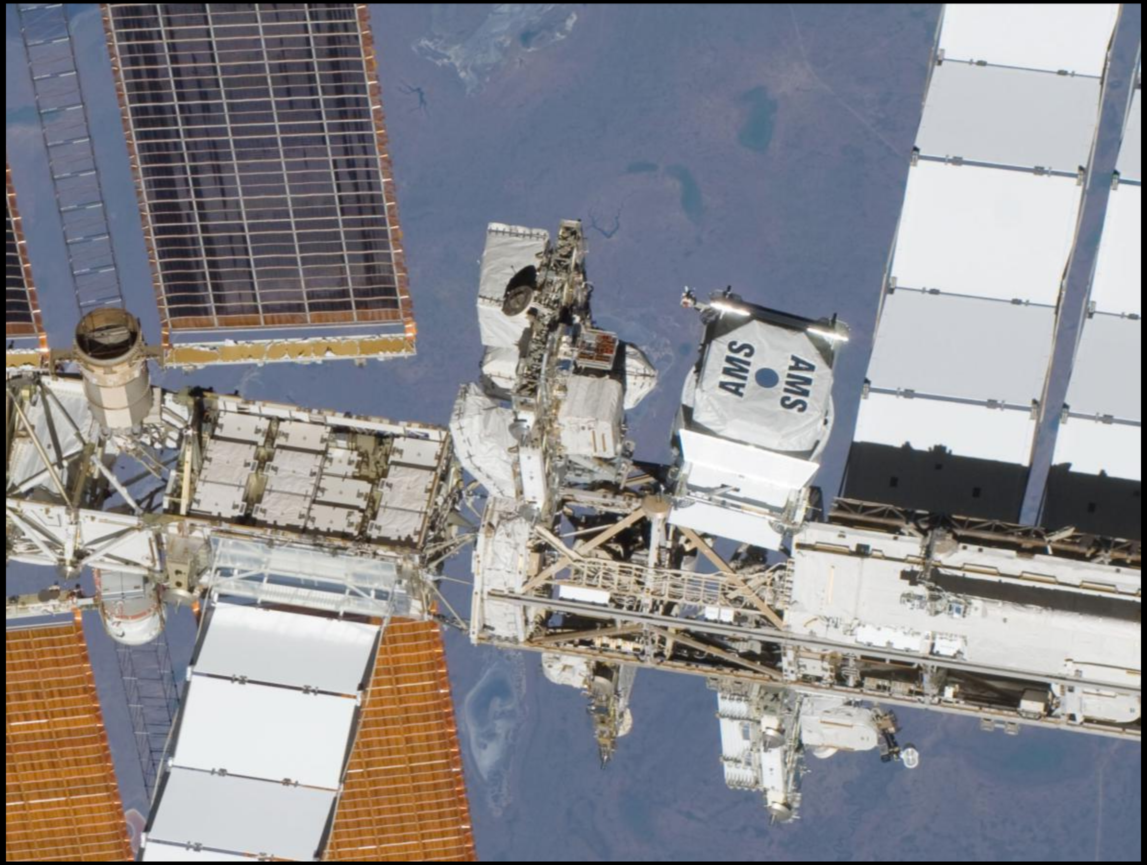

The AMS detectors provide independent information on cosmic rays

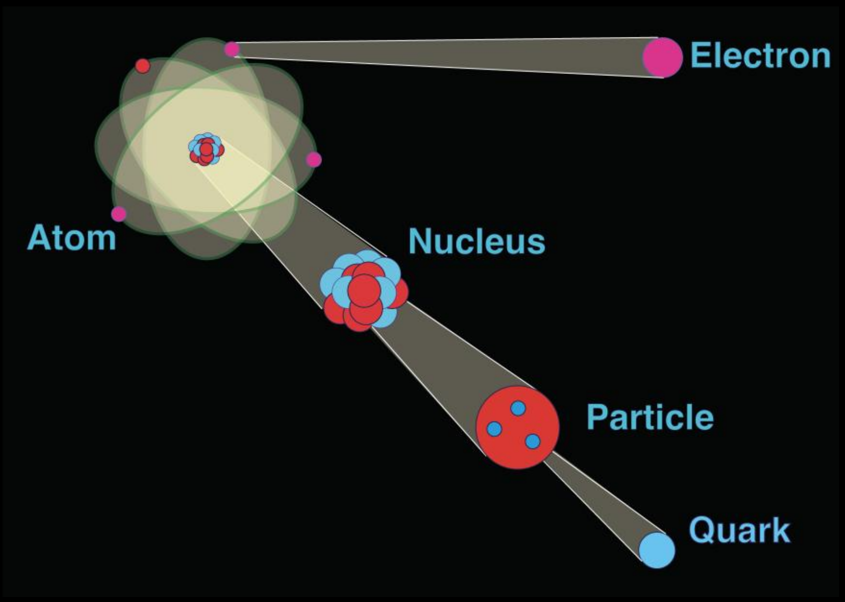

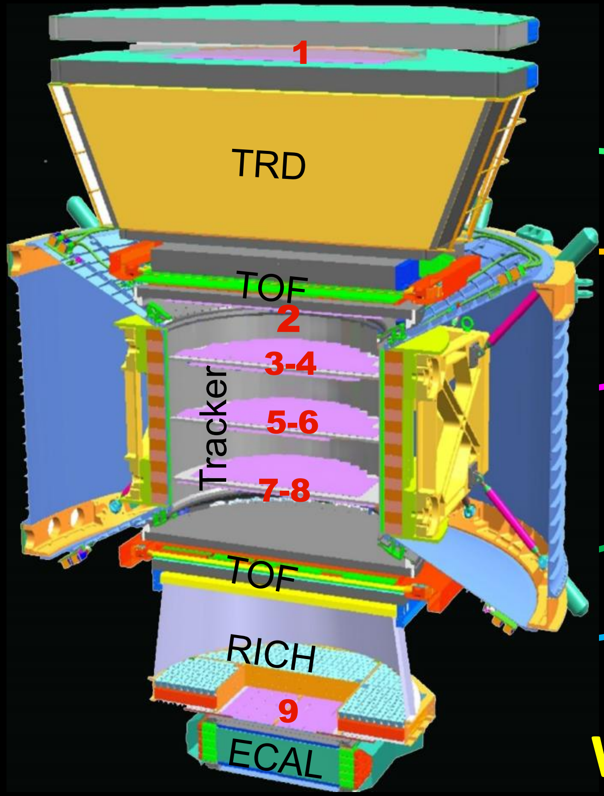

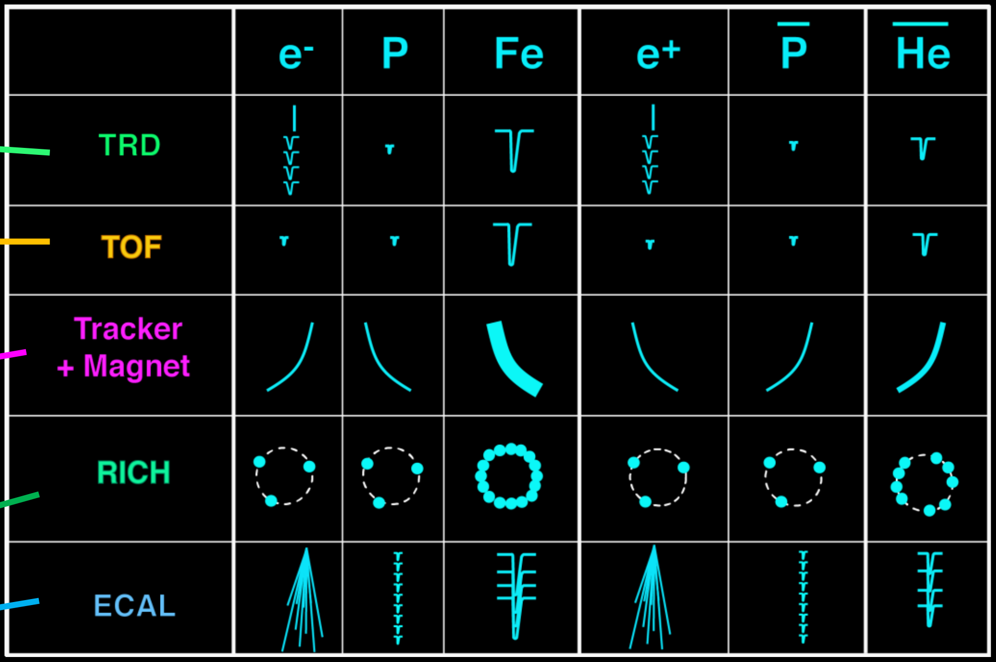

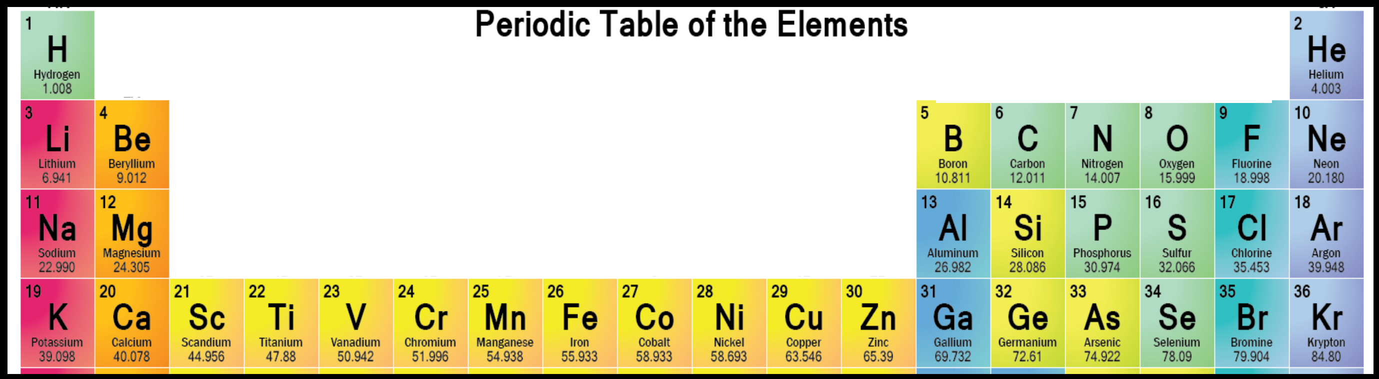

Periodic Table of the Elements

1 H Hydrogen 1.008																	2 He Helium 4.003
3 Li Lithium 6.941	4 Be Beryllium 9.012											5 B Boron 10.811	6 C Carbon 12.011	7 N Nitrogen 14.007	8 O Oxygen 15.999	9 F Fluorine 18.998	10 Ne Neon 20.180
11 Na Sodium 22.990	12 Mg Magnesium 24.305											13 Al Aluminum 26.982	14 Si Silicon 28.086	15 P Phosphorus 30.974	16 S Sulfur 32.066	17 Cl Chlorine 35.453	18 Ar Argon 39.948
19 K Potassium 39.098	20 Ca Calcium 40.078	21 Sc Scandium 44.956	22 Ti Titanium 47.88	23 V Vanadium 50.942	24 Cr Chromium 51.996	25 Mn Manganese 54.938	26 Fe Iron 55.933	27 Co Cobalt 58.933	28 Ni Nickel 58.693	29 Cu Copper 63.546	30 Zn Zinc 65.39	31 Ga Gallium 69.732	32 Ge Germanium 72.61	33 As Arsenic 74.922	34 Se Selenium 78.09	35 Br Bromine 79.904	36 Kr Krypton 84.80

With high accuracy, AMS measures

Momentum (P, GeV/c)

Charge (Z)

Rigidity (R=P/Z, GV)

Energy (E, GeV/A)

Flux (signals/(s sr m^2 GeV))

for all the charged cosmic rays, e+, e−, p, and $\bar{p}$,

and the nuclei in the Periodic Table

AMS-02 Layer0 Tracker

- A new silicon strip tracker(Layer0) on the top of AMS-02
  - Larger sensitive area (~7m^2)
- 8/10/12 SSDs are connected in series to form a ladder
  - Large detection area with small **power consumption**
  - Each readout channel corresponds to a very long (~1m) strip
  - Requires high precision placement(<5 um) of the SSDs on the ladder, and precise SSD alignment after assembly with beam

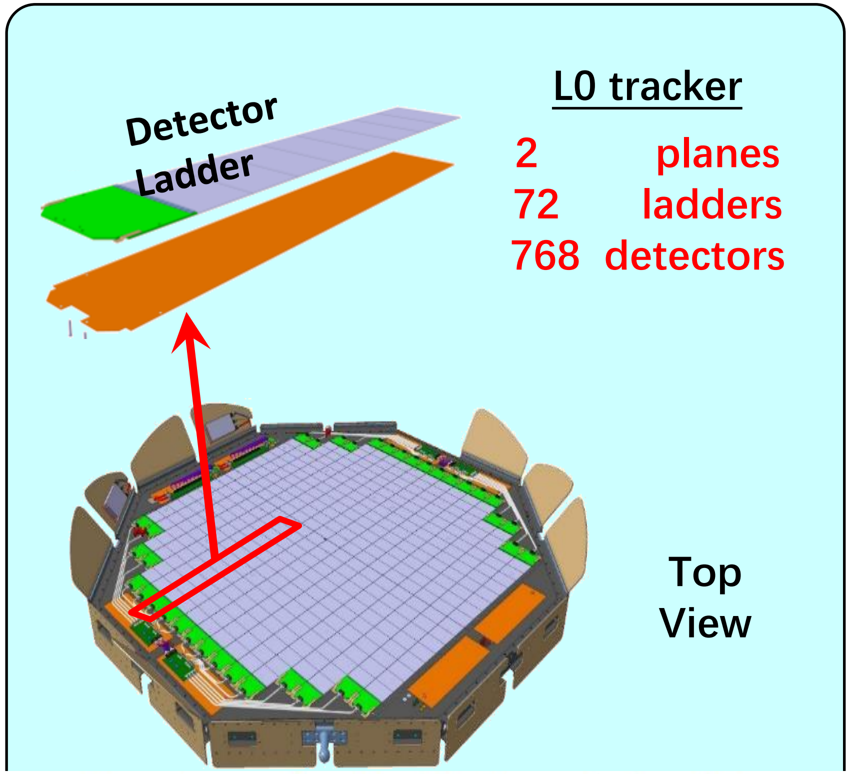

New Layer 0 added to the existing 9 Layers

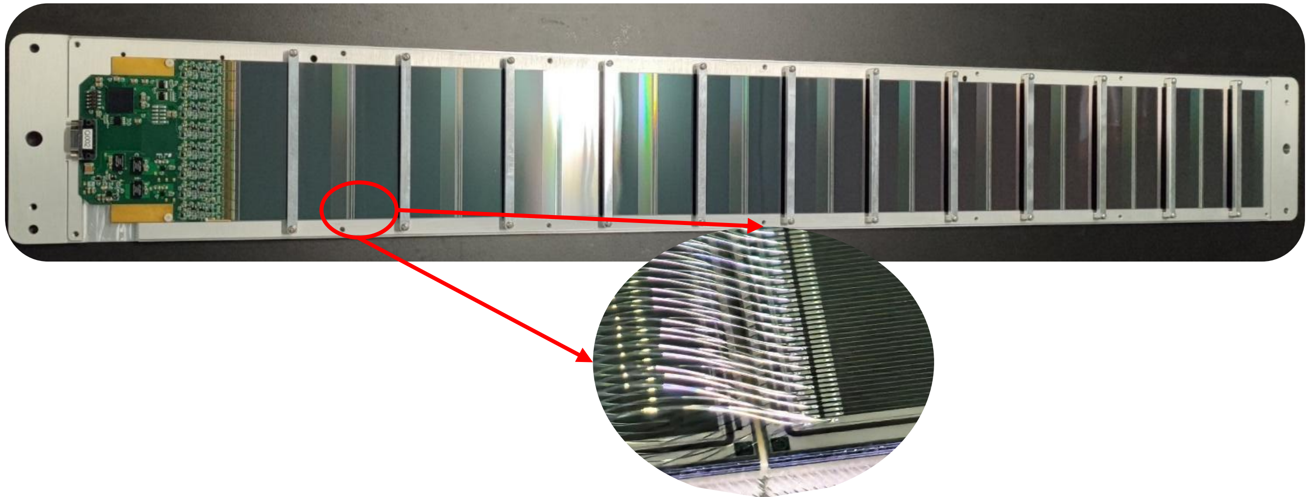

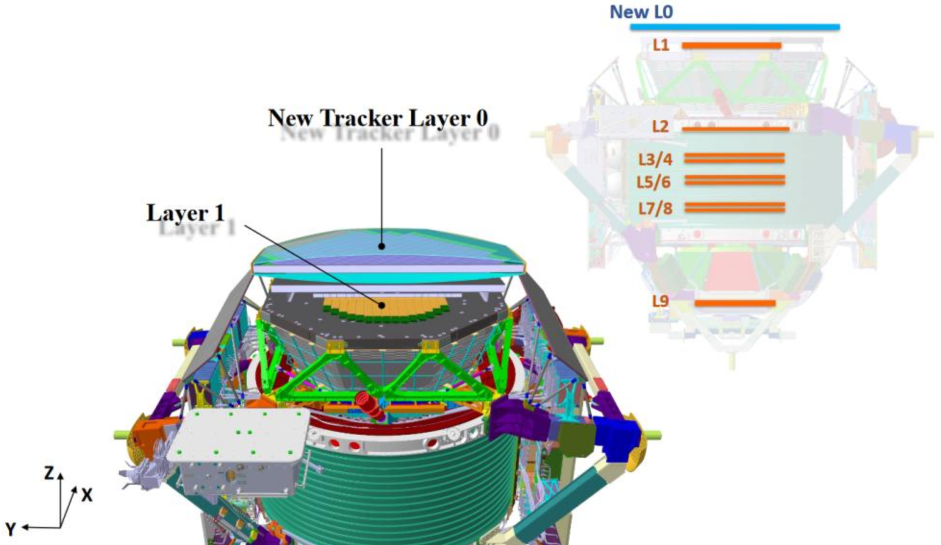

Detector construction in IHEP

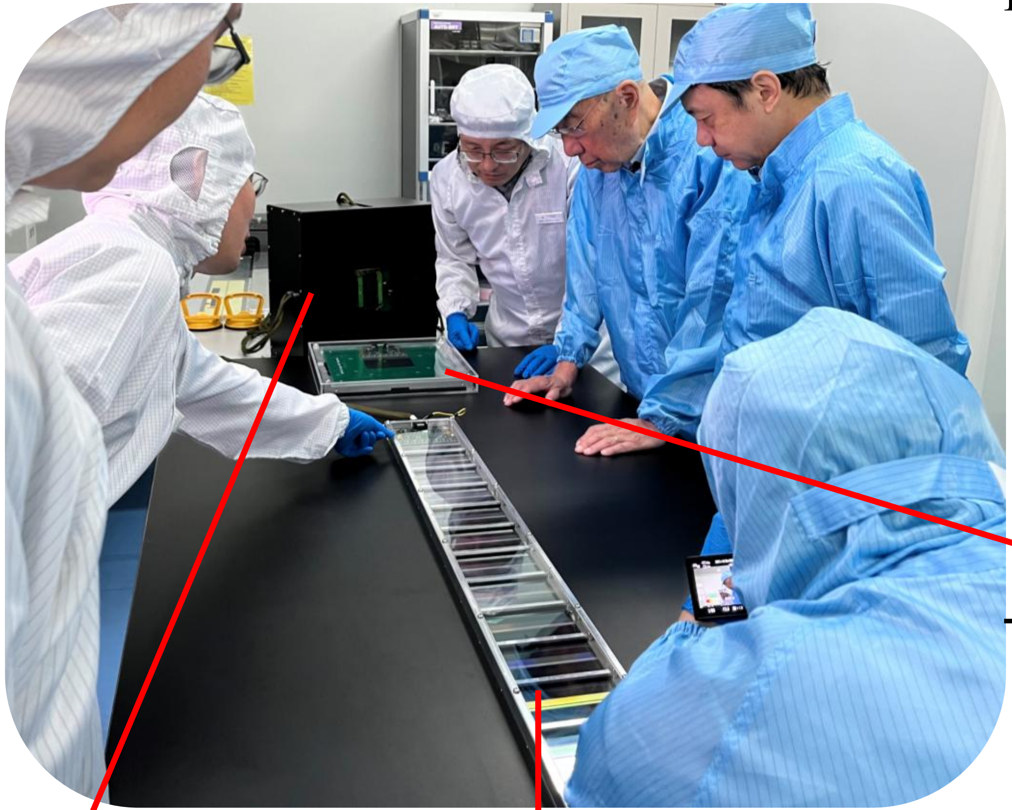

Beam Telescope

Detector module (ladder)

Telescope Board

Electronics by MIT

SSD by IHEP

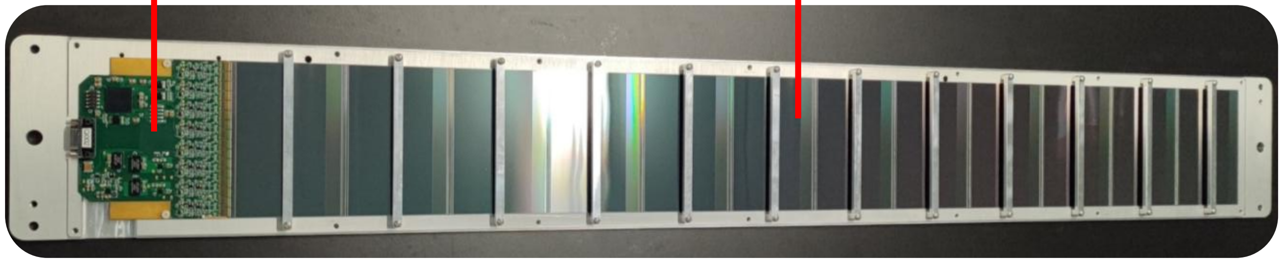

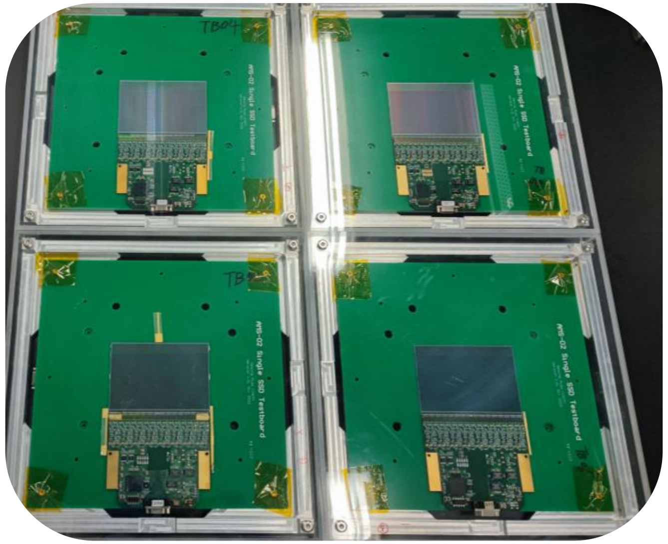


AMS L0 Upgrade Module Production
Successfully completed
October 21 2024
FILA

Detector construction in Europe

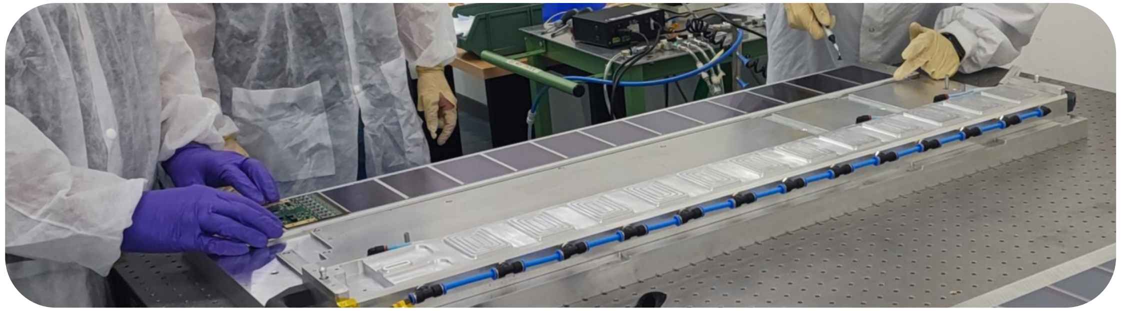

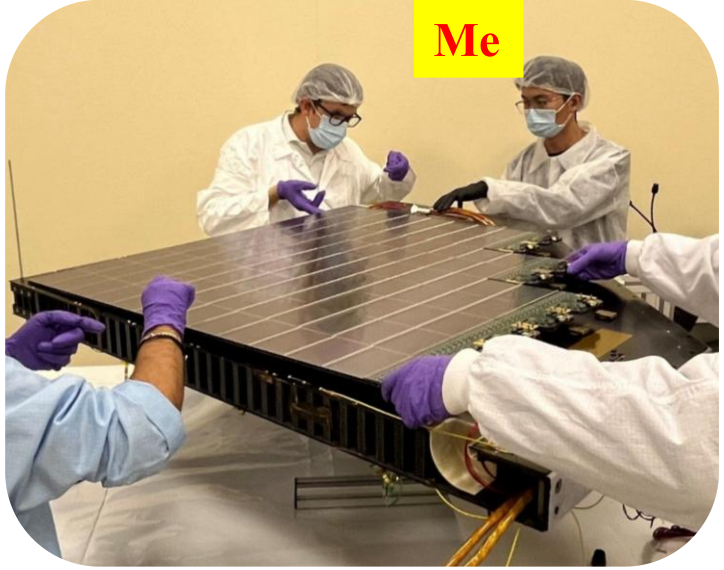

Ladder reception and ¼ Layer assembly in Italy

Full Layer assembly in CERN

Joining in space Qualification in Italy

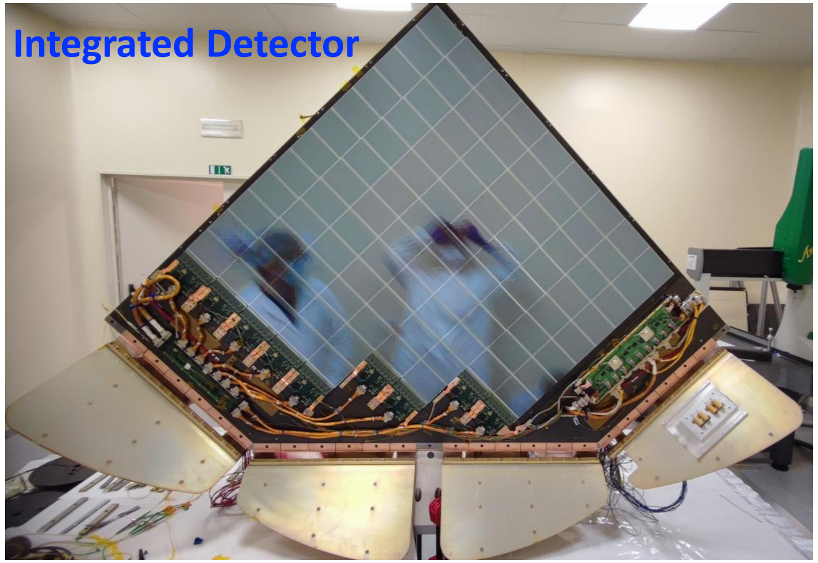

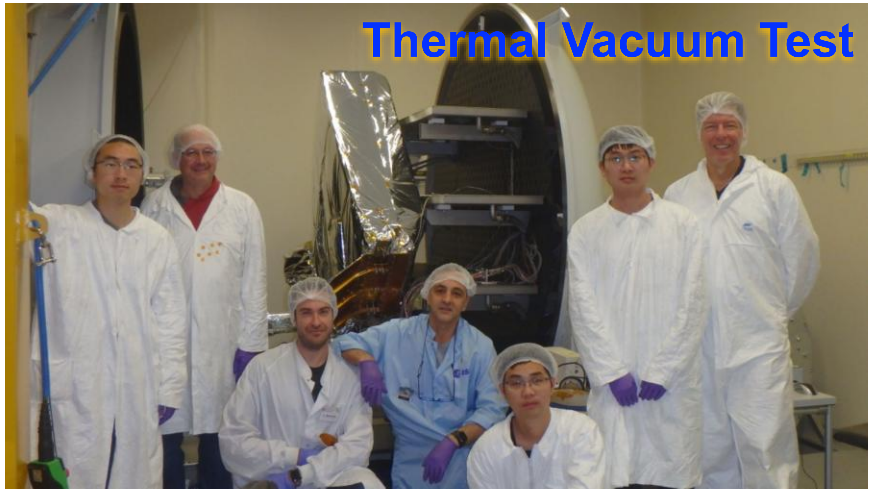

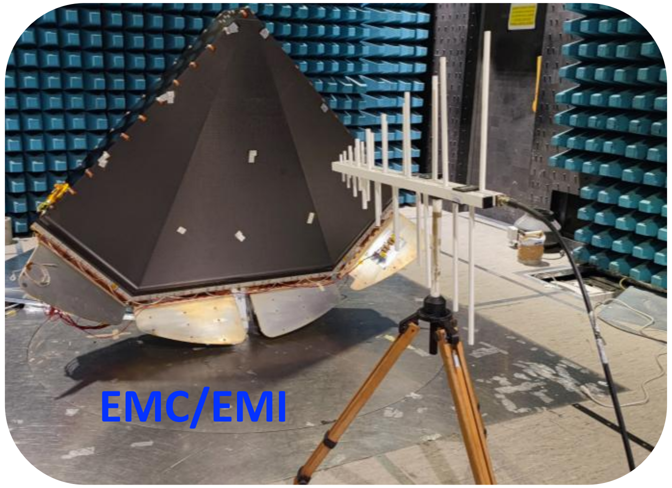

Detector performance study

Design of the silicon strip sensor

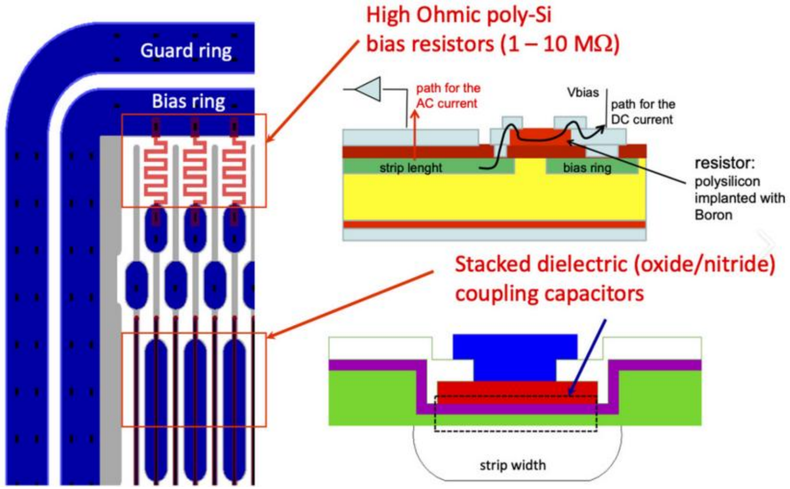

A typical AC-coupled silicon microstrip sensor

- Every strip AC-coupled to readout
- Small bias resistor

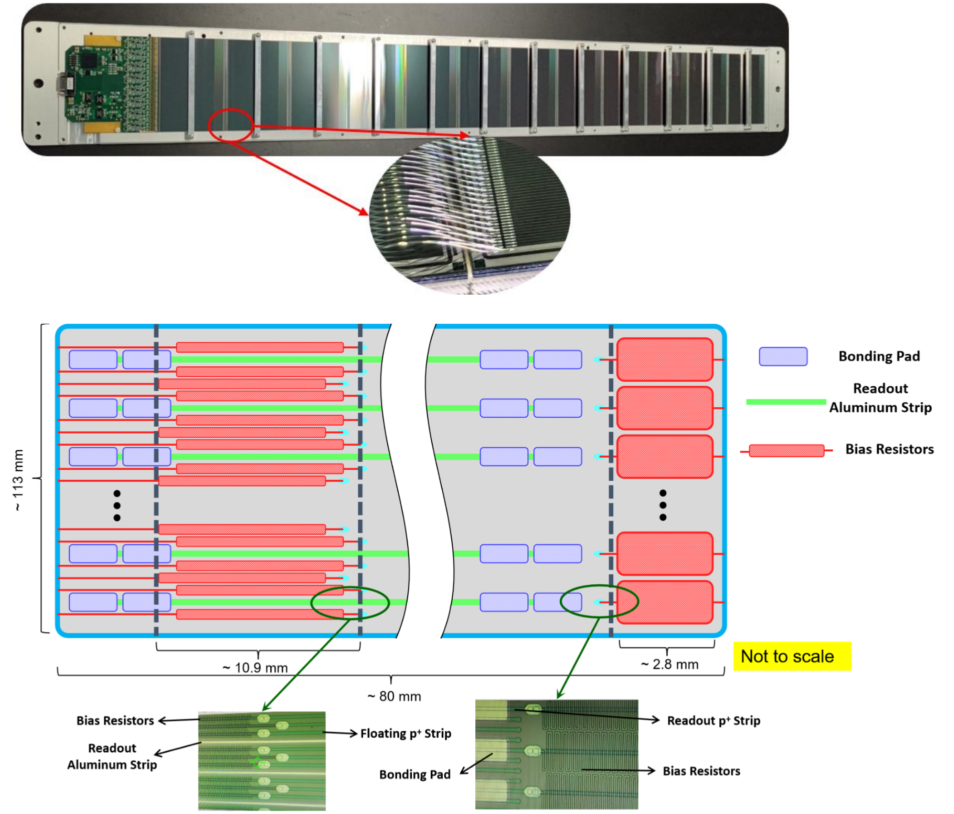

Limited power consumption

- Long daisy chain => large bias resistor (~100MΩ)
- 3 floating strips

Design of the silicon strip sensor

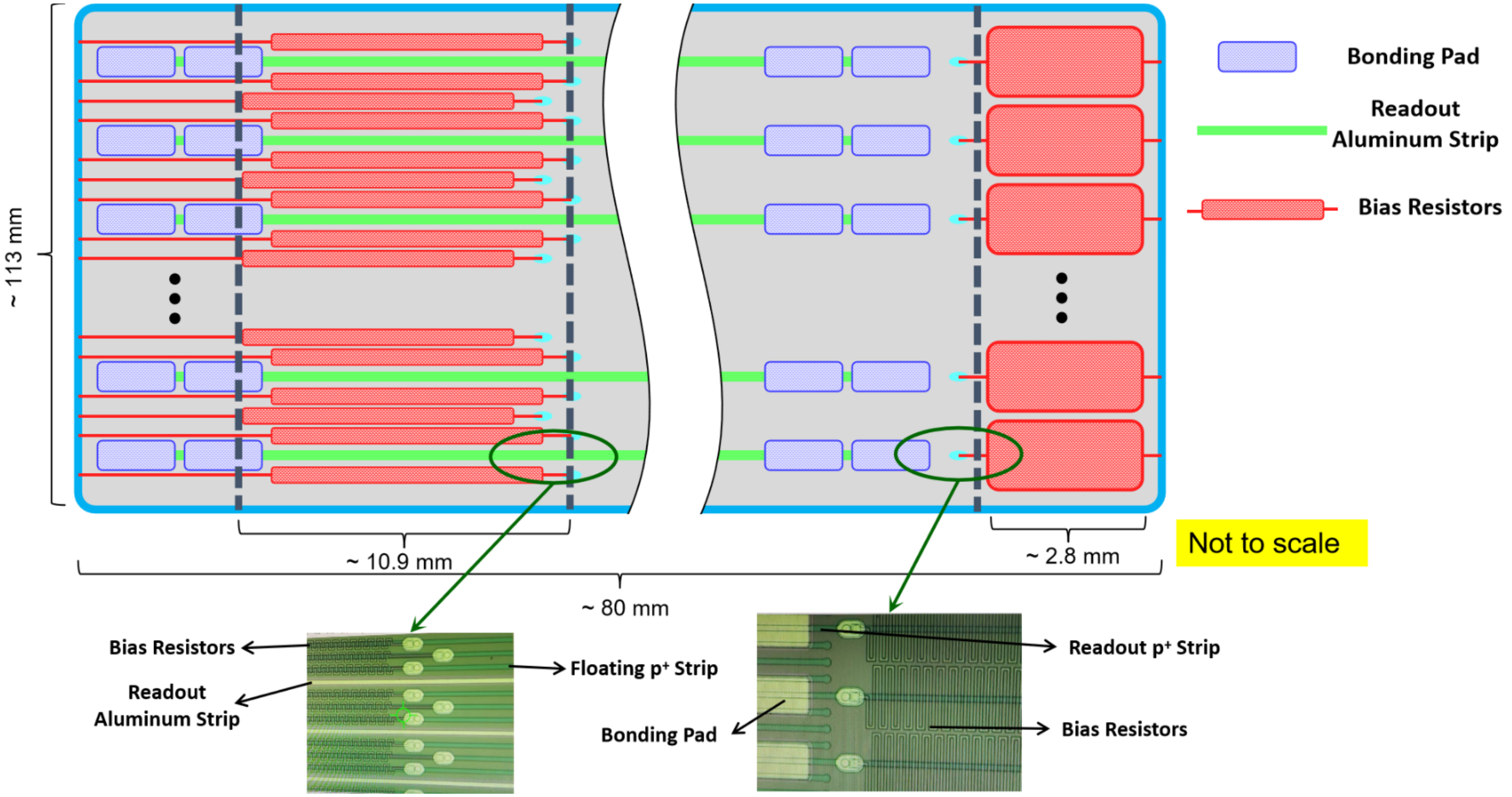

- Readout pitch 109um with 3 floating strips => spatial resolution?
- Insert bias resistors of floating strips between 2 readout aluminum strip => affect efficiency ?

Verification by beam test

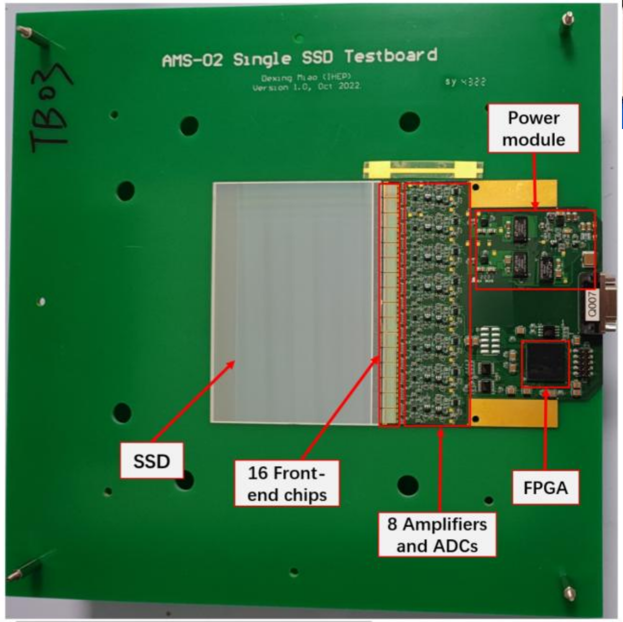

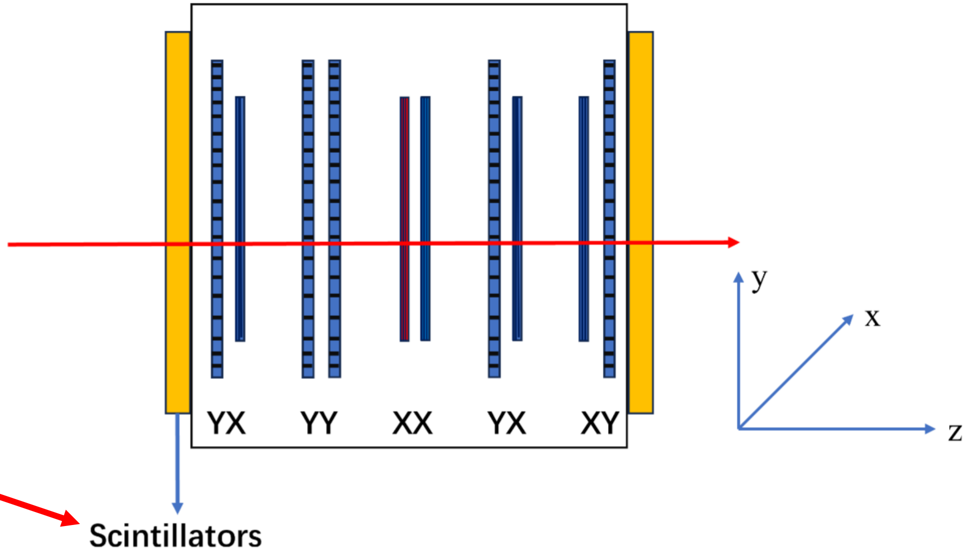

- 8cm * 14cm trigger region, cover the full sensor along strip direction

Detector alignment

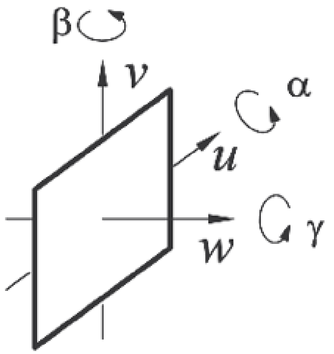

Alignment : Optimize the correction parameters to minimize the chi2

$$\chi^2(\Delta\mathbf{p},\Delta\mathbf{q}) = \sum_j^{\text{tracks}} \sum_i^{\text{meas.}} \frac{r_{ij}^2}{\sigma_{ij}^2}$$

i:detector
j:track

which

$$r_{ij} = m_{ij} - f_{ij}(\mathbf{p}_0,\mathbf{q}_{j0}) - \frac{\partial f_{ij}}{\partial \mathbf{p}}\Delta\mathbf{p} - \frac{\partial f_{ij}}{\partial \mathbf{q}_j}\Delta\mathbf{q}_j$$

$\vec{p}$: detector correction parameters
$\vec{q}$: track fit parameters

At local system, with 6 correction parameters (Δu,Δv,Δw,α,β,γ):

$$\mathbf{J} = \begin{pmatrix} -1 & 0 \\ 0 & -1 \\ \tan\psi & \tan\vartheta \\ v_x \tan\psi & v_x \tan\vartheta \\ u_x \tan\psi & u_x \tan\vartheta \\ v_x & -u_x \end{pmatrix}$$

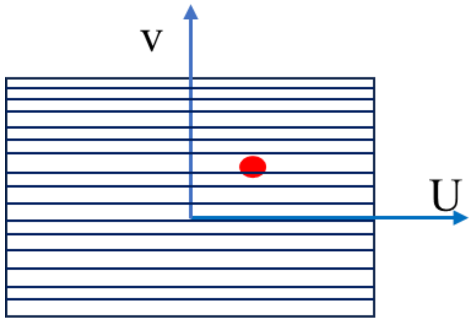

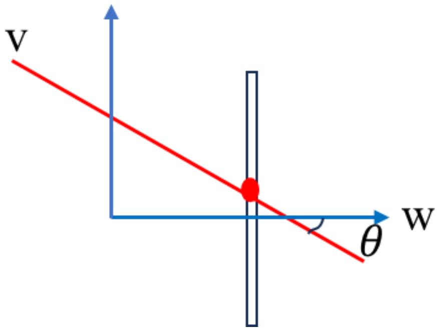

- 3-D track is necessary, even though we have only 1-D detection

Millepede-II V04-16-00

Hit position reconstruction => double-η

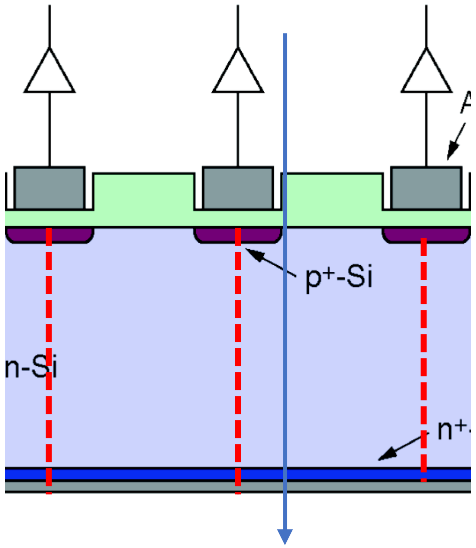

$$X_{COG} = \sum_{cluster} S_i x_i \Big/ \sum_{cluster} S_i ,$$

$$\eta = \frac{S_R}{S_R + S_L},$$

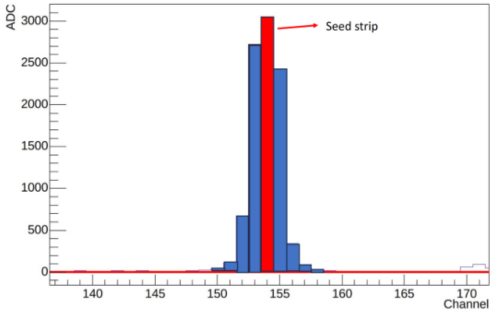

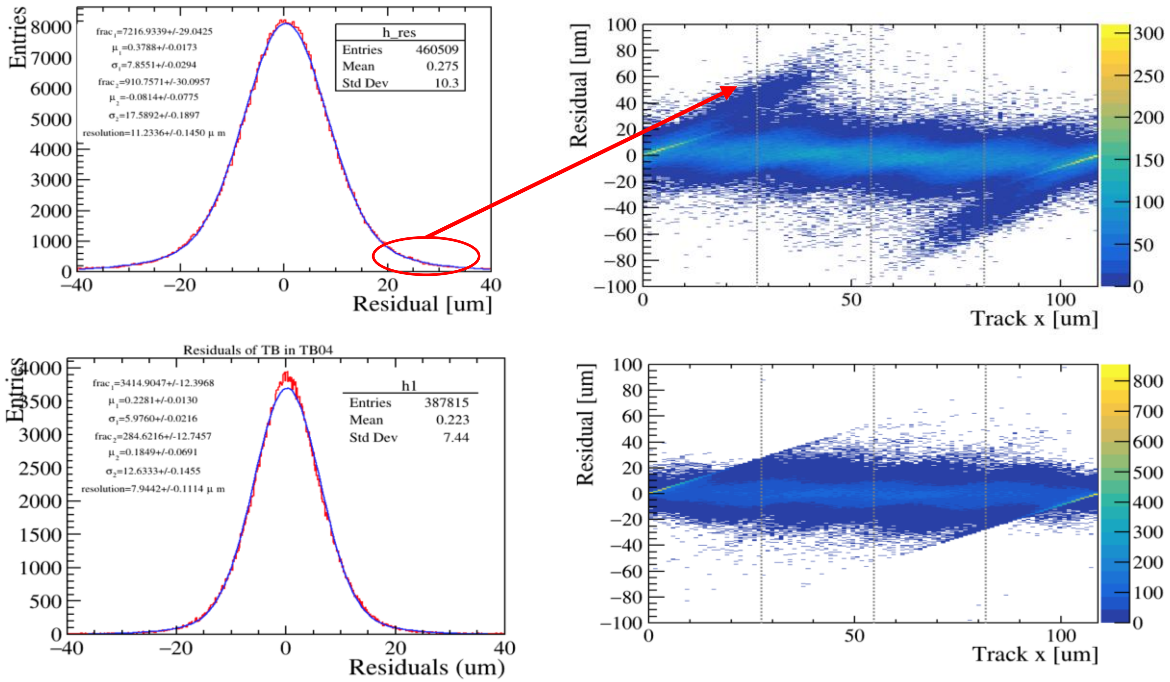

- Charge sharing between strips is nonlinear, the eta algorithm can reflect this nonlinearity [Nucl.Instrum.Meth.A 335 (1993) 44-58]
- When the detector noise causes the signal size to flip, there will be a large deviation
  - Double-η algorithm was developed to correct

SSD Performance Results

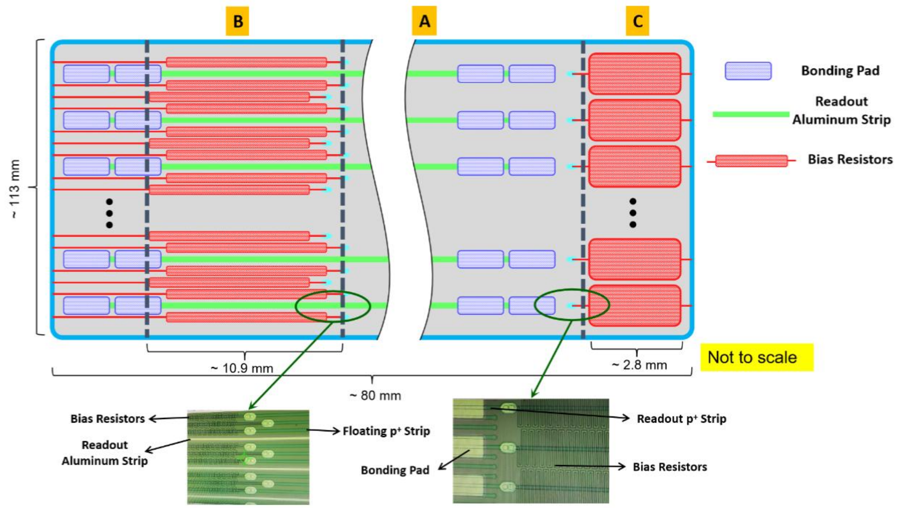

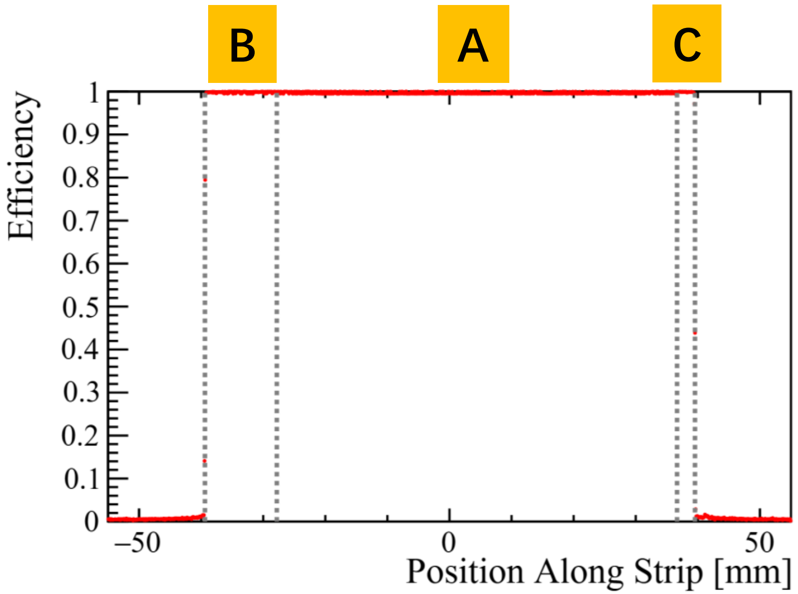

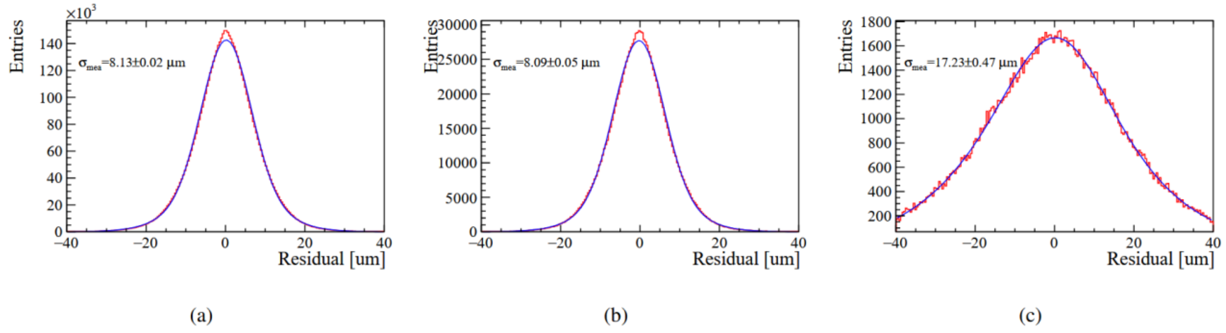

- The presence of the bias resistor does not lead to a decrease in detection efficiency and position resolution
  - Total efficiency of single layer is 99.8%
- Adding 3 floating strips can improve the spatial resolution from 17um to 8um
  - Enhance charge sharing, increase the proportion of cluster size >1

Enhancement of charge sharing by bias resistors

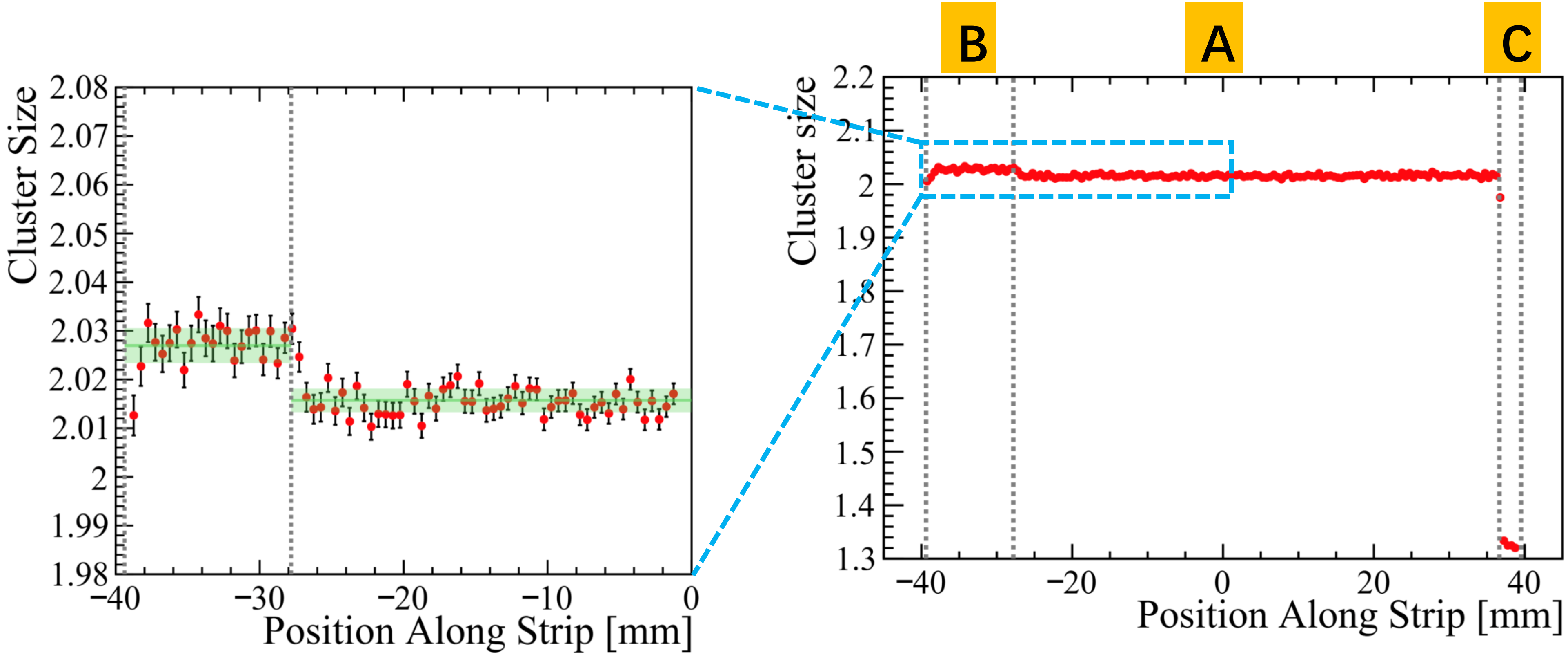

- Observed the presence of the bias resistor does not lead to a decrease in detection efficiency and position resolution
- Accepted by Nucl.Sci.Tech, 2505.23050 **[First author]**

Heavy nuclei cosmic ray performance study

Heavy Ion beam test @SPS

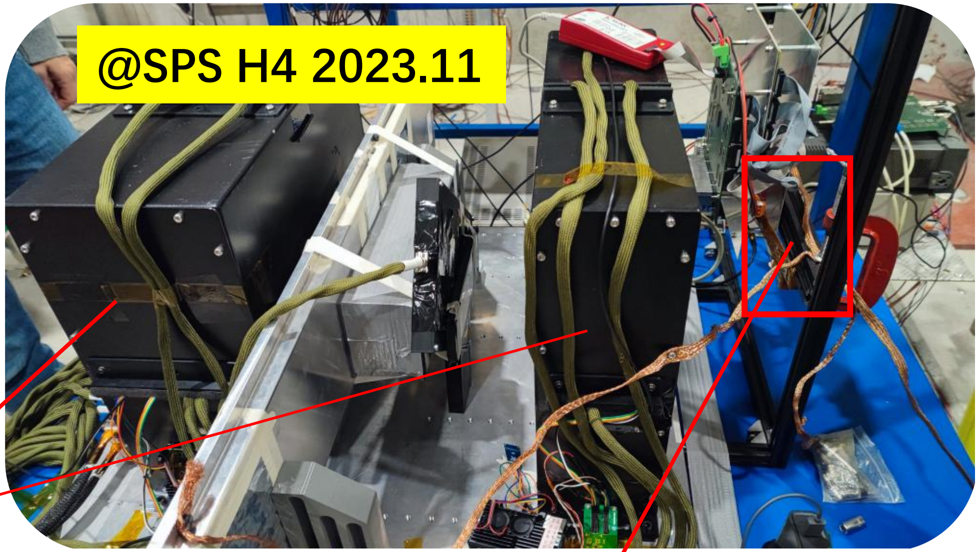

Beam Monitor

Charge tagger detector

- Using a mixed beam produced by target firing of a 120 GeV/n primary Pb beam
  - Use a charge tagger detector to give a charge reference of every event
- Study the PID and tracking performance of Beam Monitor and ladder (by INFN colleagues)
- Developing a new heavy-nuclei PID algorithm

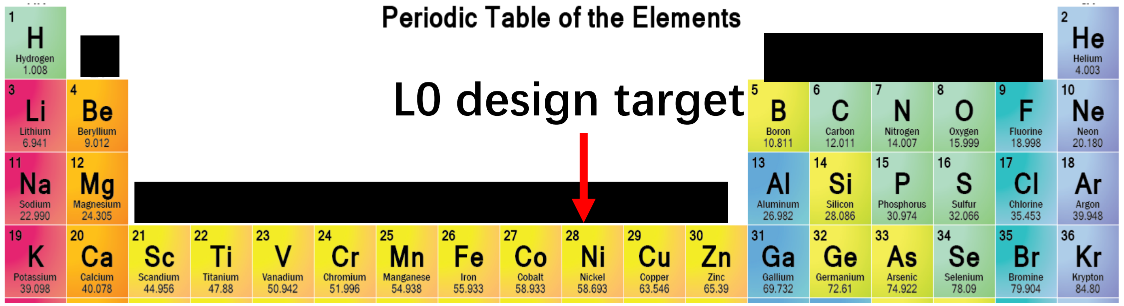

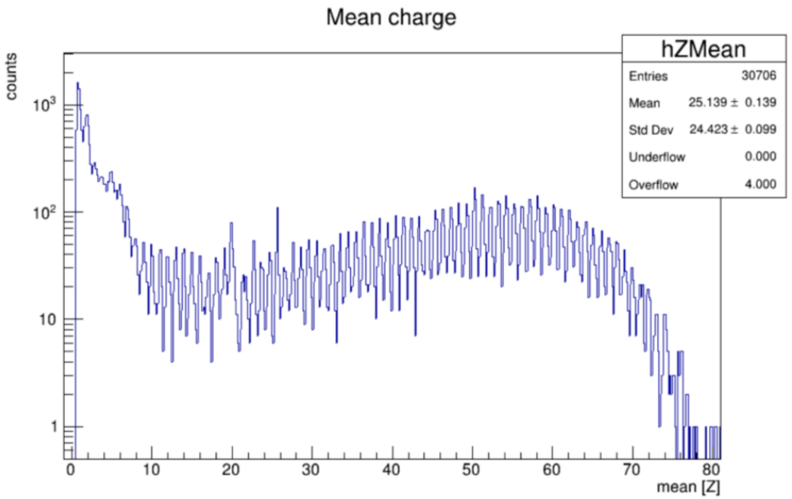

Particle idenatification based on BDT

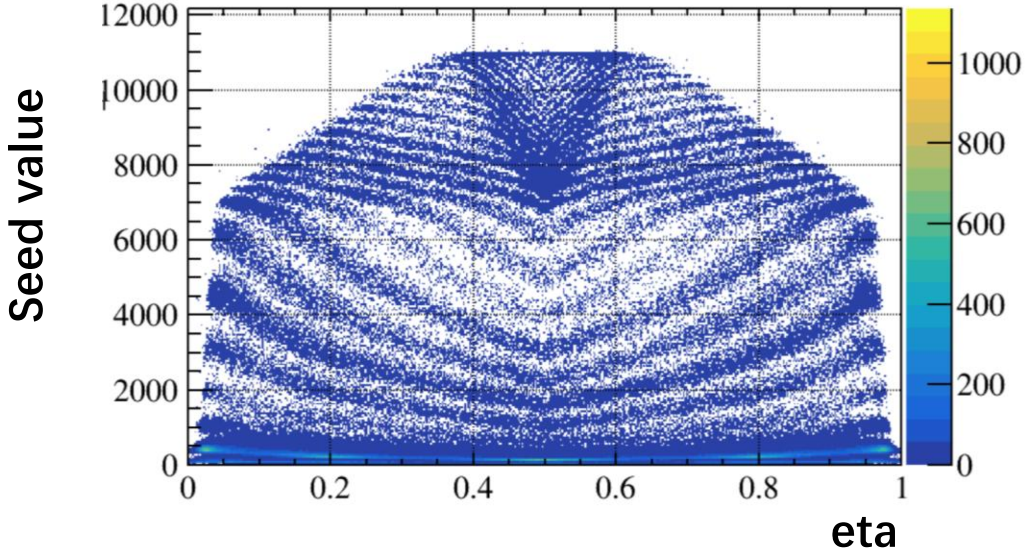

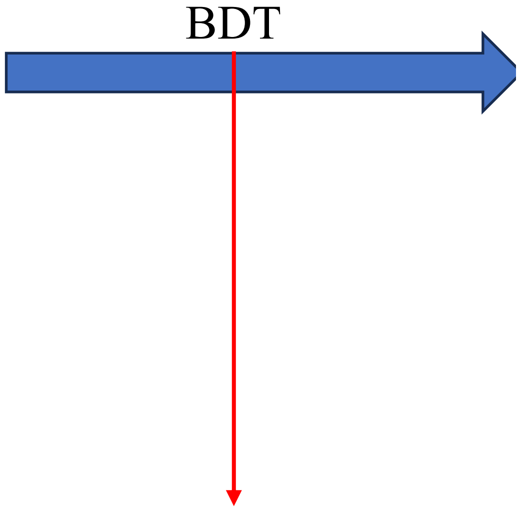

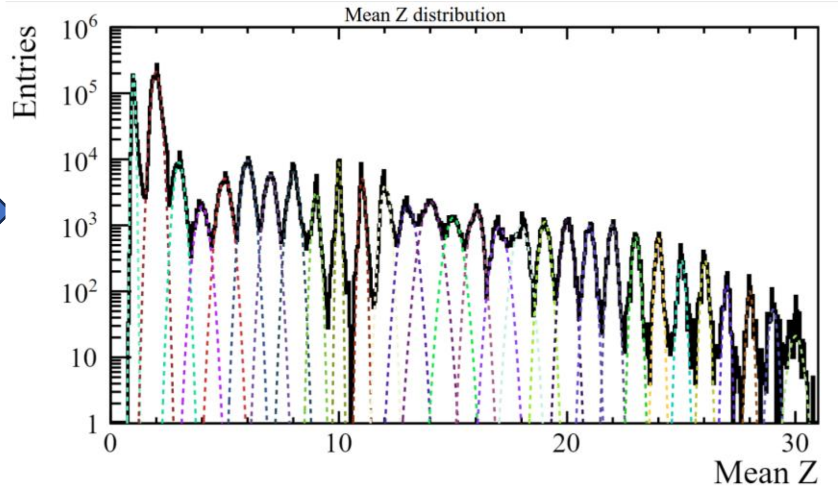

- Output: Z value of the event

Input: signal value of every channels in a cluster of a heavy ion event

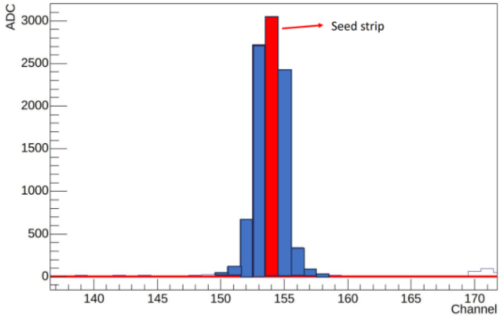

- Use 3 channels of each cluster
  - [seed-1, seed, seed+1]

- Implementing independent PID
- Multivariate problems are well suited for BDT regression
- Only the training set requires labeled data => no MC samples, need to build a training set

Tracking based on Z-tag

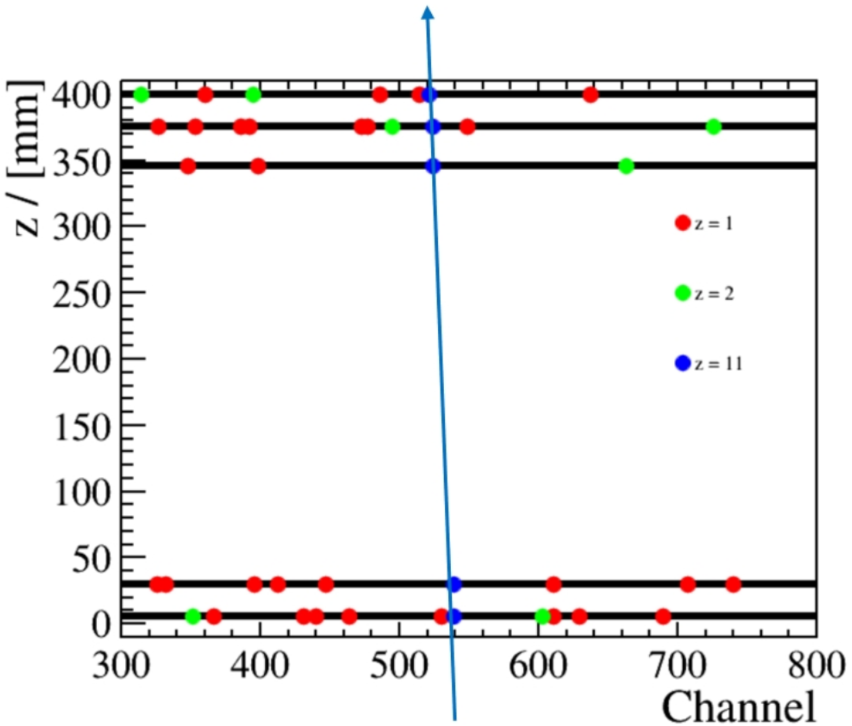

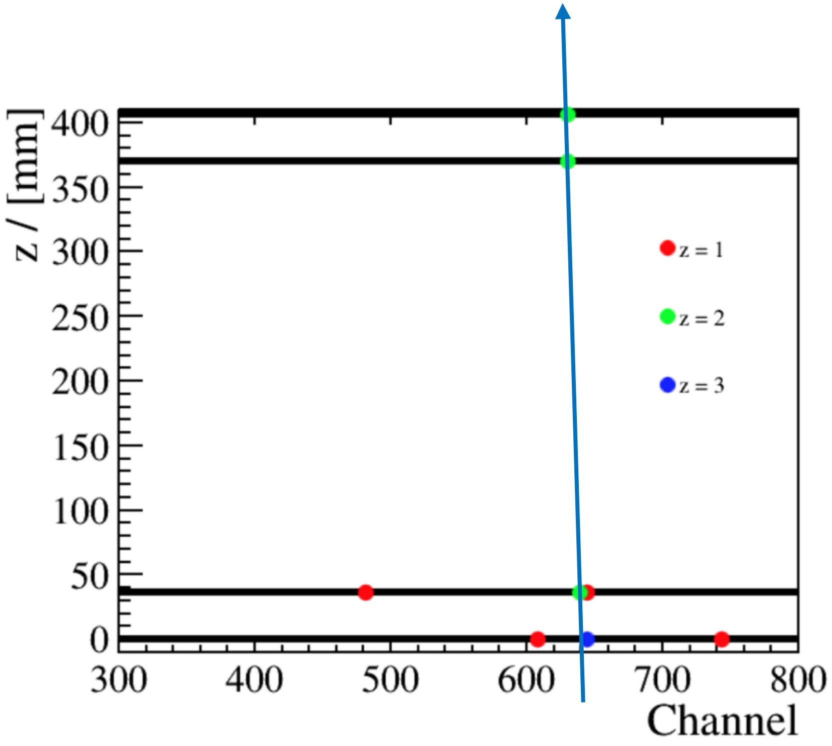

- Tracking process:

1. Find the maximum z in an event as the particle to be tracked
2. Find the hits in the range [z-1,z+1] in all layers
3. Select the track with the smallest chi2dof

Charge resolution results

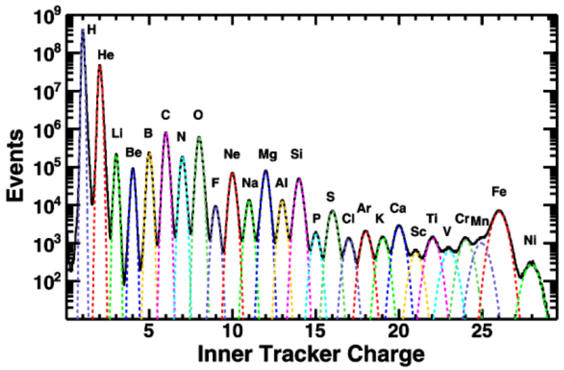

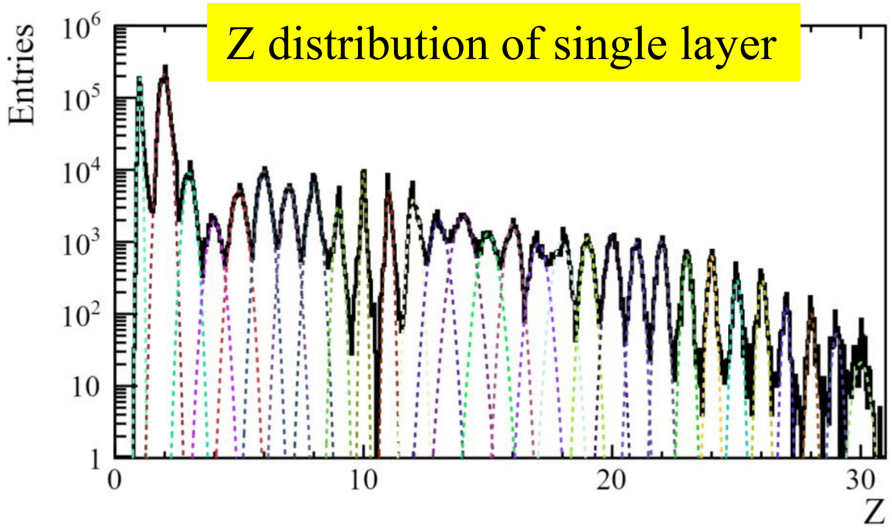

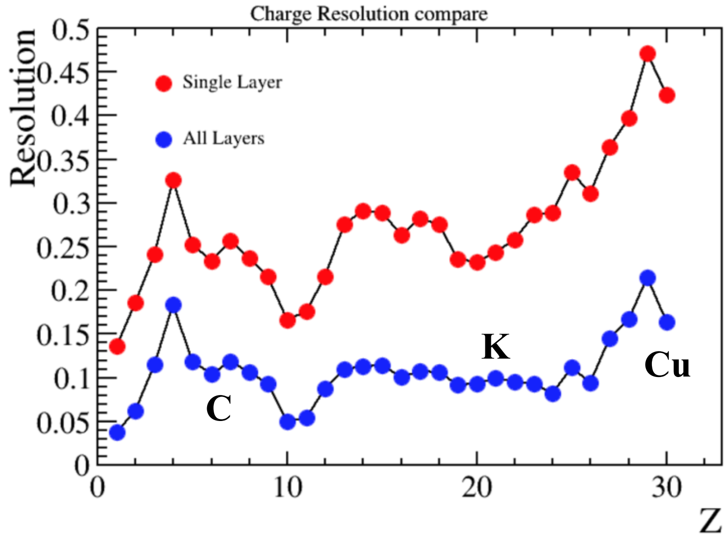

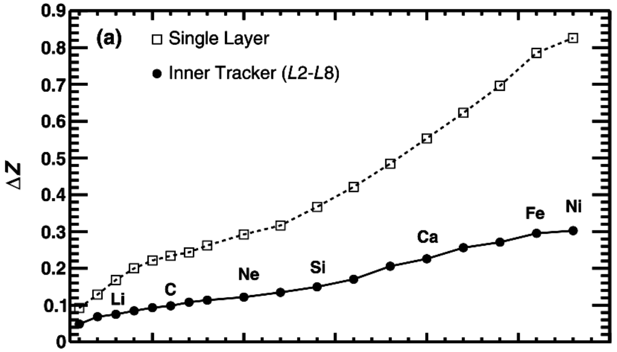

Fig. 17. (a) Charge resolution ΔZ and (b) $\Delta Z/Z$ of the inner tracker (circles) and a single layer (squares) as functions of nuclei charge Z with rigidity > 7 GV. As seen in (b), $\Delta Z/Z$ is approaching a constant value ~0.01 for high Z.

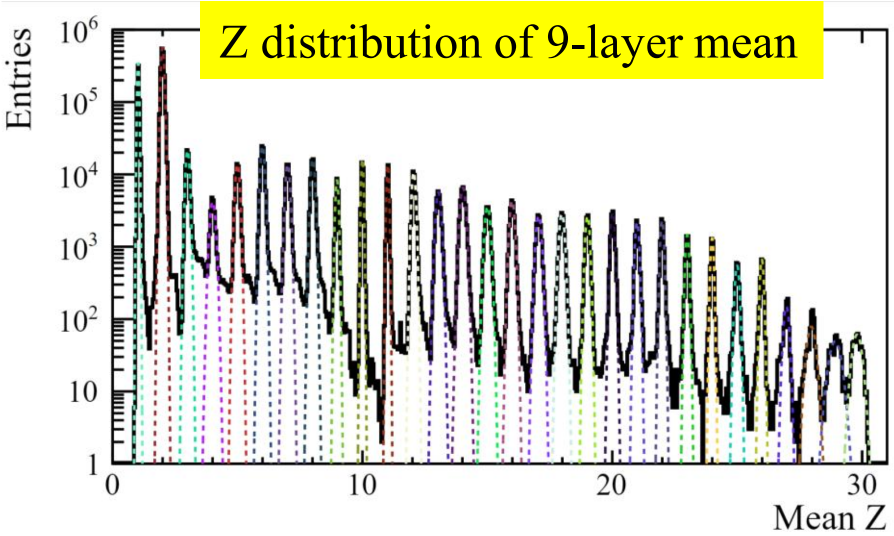

- After tracking, can calculate mean Z of all 9 layers of each track
- Get charge resolution of single layer and 9-layer telescope up to Cu(Z=30) nuclei
  - For telescope, get ~0.1 charge unit resolution for most nuclei
  - Significantly better charge resolution than AMS-0

Heavy nuclei performance

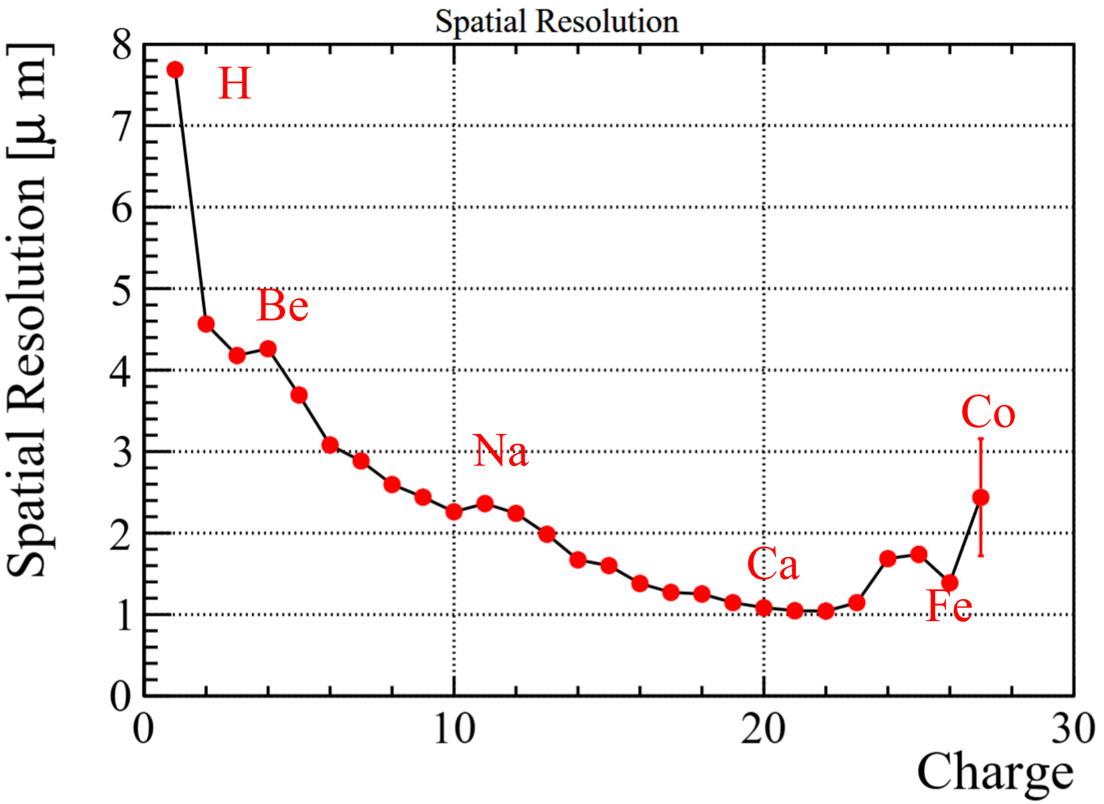

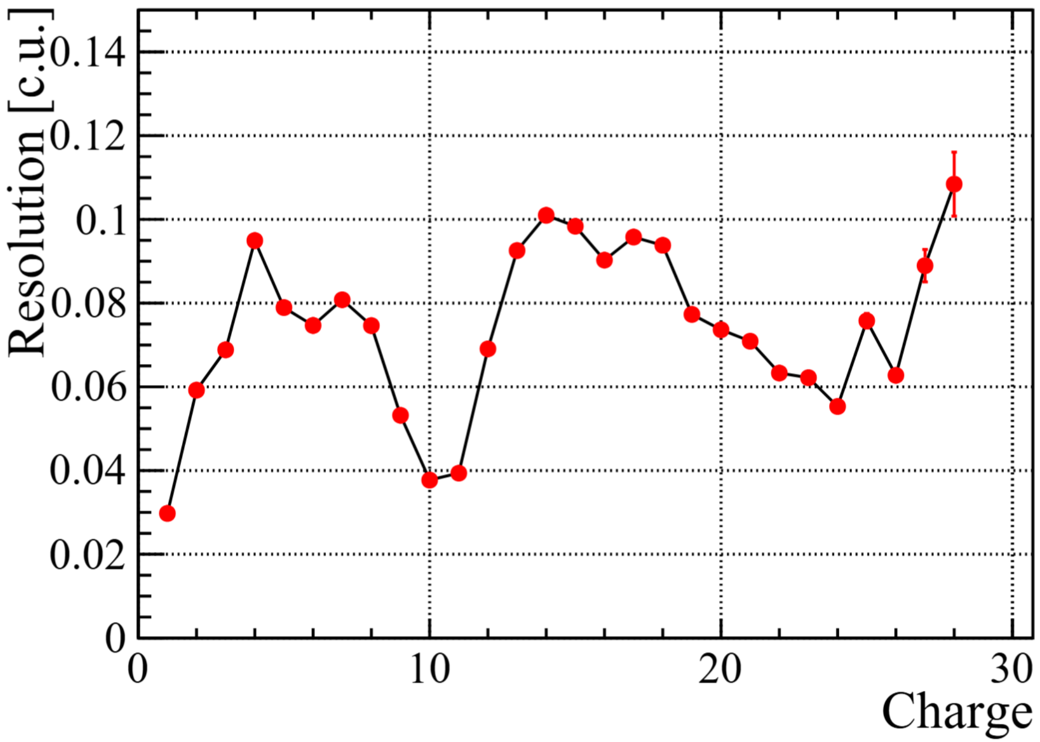

- Charge resolution ~0.1, up to Z=29, position resolution best 1um
- **To be submitted to NIMA in the next month [First author]**

A 4D Telescope System for Charge and Position Measurement of High Energy Nuclei

Dexing Miao[a,b], Zhiyu Xiang[a], Jianchun Wang[a], Pingcheng Liu[d], Xudong Cai[c], Hsin-Yi Chou[f], Mingjie Feng[a,b], Liangchenglong Jin[a], Vladimir Koutsenko[c], Qinze Li[a,b], Cong Liu[d], Zibing Wu[e], Xuhao Yuan[a], Xiyuan Zhang[a], Zijun Xu[a,*]

[a]*Institute of High Energy Physics, Beijing 100049, China*
[b]*University of Chinese Academy of Sciences, Beijing 100049, China*
[c]*Massachusetts Institute of Technology (MIT), Cambridge, Massachusetts 02139, USA*
[d]*Shandong Institute of Advanced Technology, Jinan 250100, China*
[e]*Shandong University (SDU), Jinan, Shandong 250100, China*
[f]*Institute of Physics, Academia Sinica, Nankang, Taipei, 11529, Taiwan*

Unsupervised Learning Algorithm for Heavy-nuclei PID

Why unsupervised learning ?

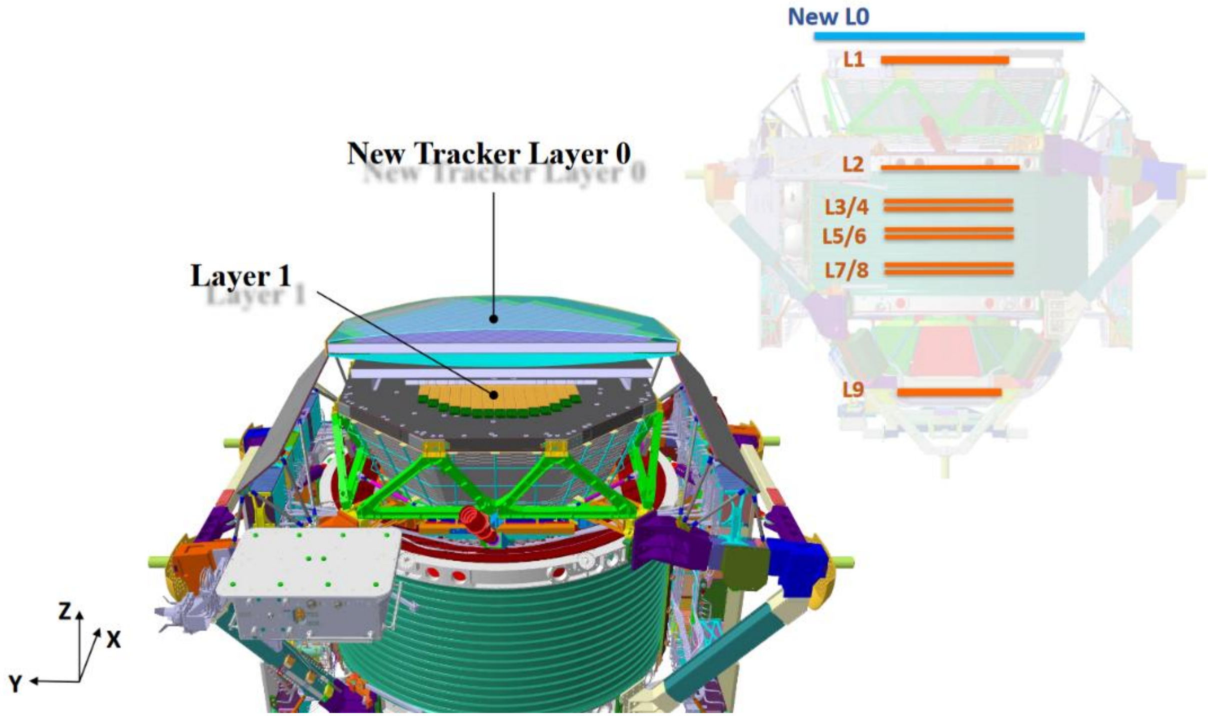

- Independent of MC and other detectors
- L0 on the top of AMS with the largest acceptance, without relying on other detector tags will enhance AMS physics reach

- Unsupervised learning is widely applied across physics, and advancing its techniques enables broad applications
  - Identifying topological order [Nature Physics, 790–795 (2019)]
  - Learning phase transitions [Nature Physics, 435–439 (2017)]
  - Search for New Phenomena at ATLAS [PhysRevLett.132.081801]
  - Anomaly Detection for Resonant New Physics [PhysRevLett.121.241803]
  - Study about Anomaly Detection / jet tag [JHEP, 2022, JHEP, 2025 ....]

Basic idea of unsupervised implementation

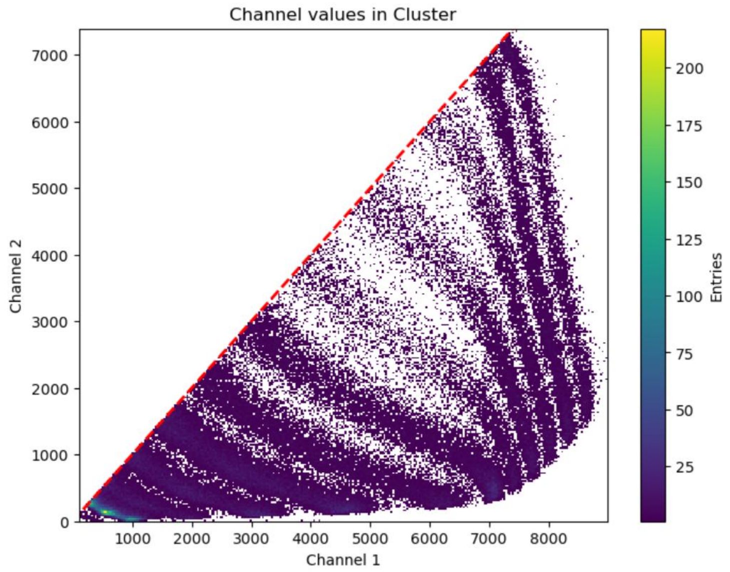

- A particle hitting the silicon strip detector forms a cluster, whose shape and size depend only on two factors: **hit position and particle charge**
- In high-dimensional space, clusters are distributed as multi-layered, complex surfaces
    - Use NN to learn these structure

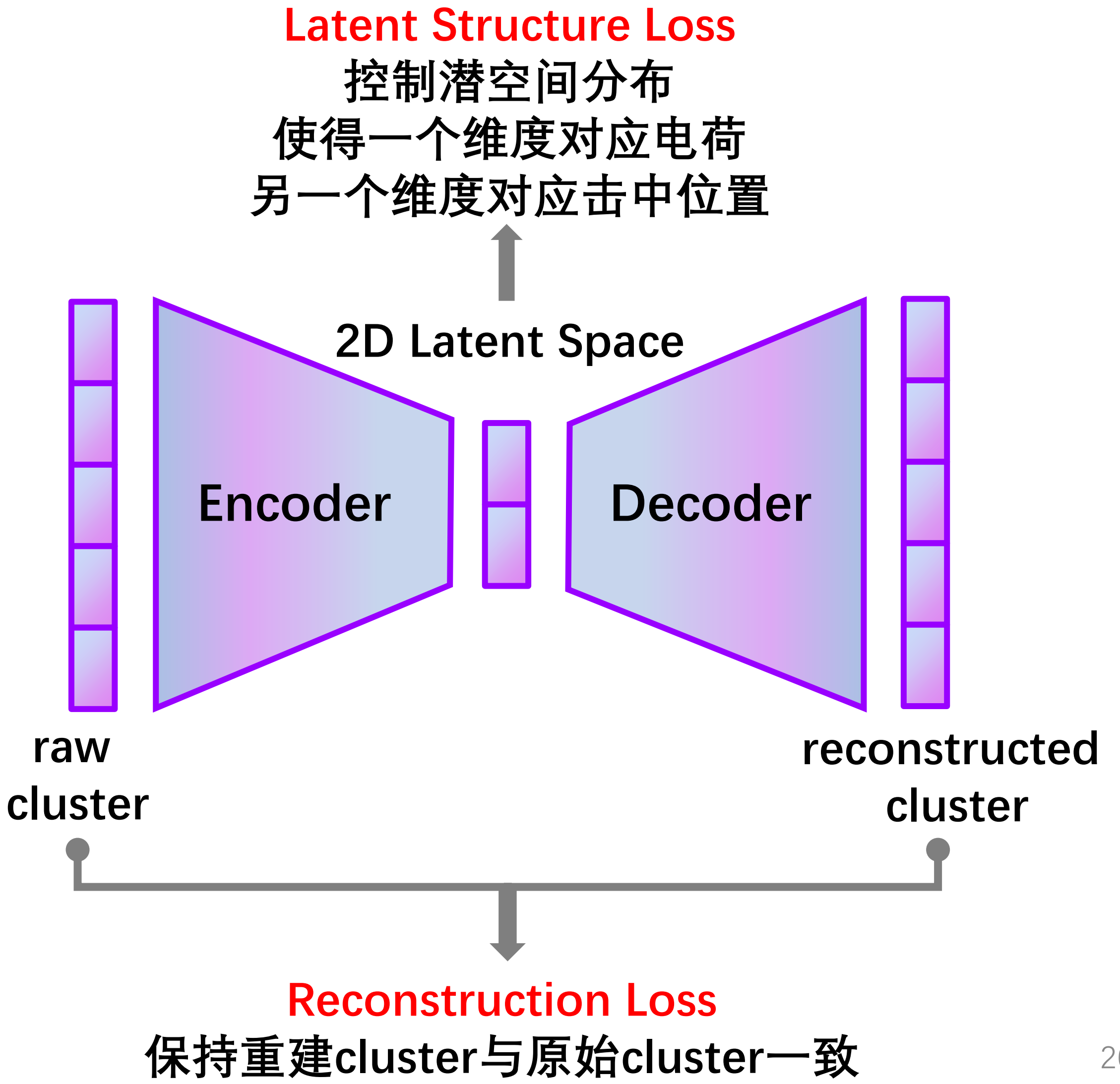

Challenges: Precise control of latent space

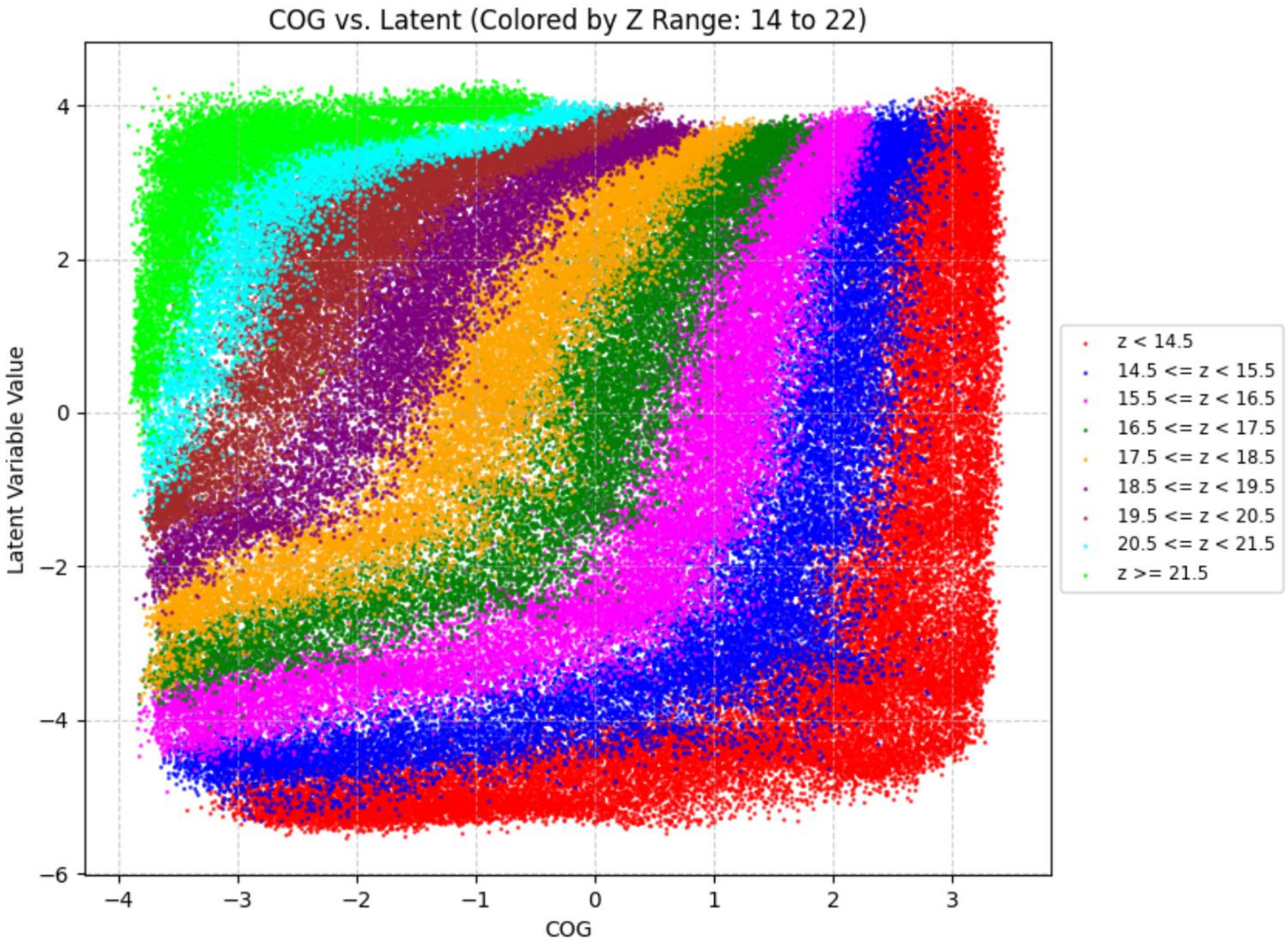

- Cluster shape is determined by charge & hit position, but arbitrary one-to-one mappings (linear or nonlinear) can also reconstruct clusters
- Reconstruction loss alone cannot ensure latent dimensions correspond to physical quantities

Solution: Precise control of latent space

Our solution: Histogram Loss

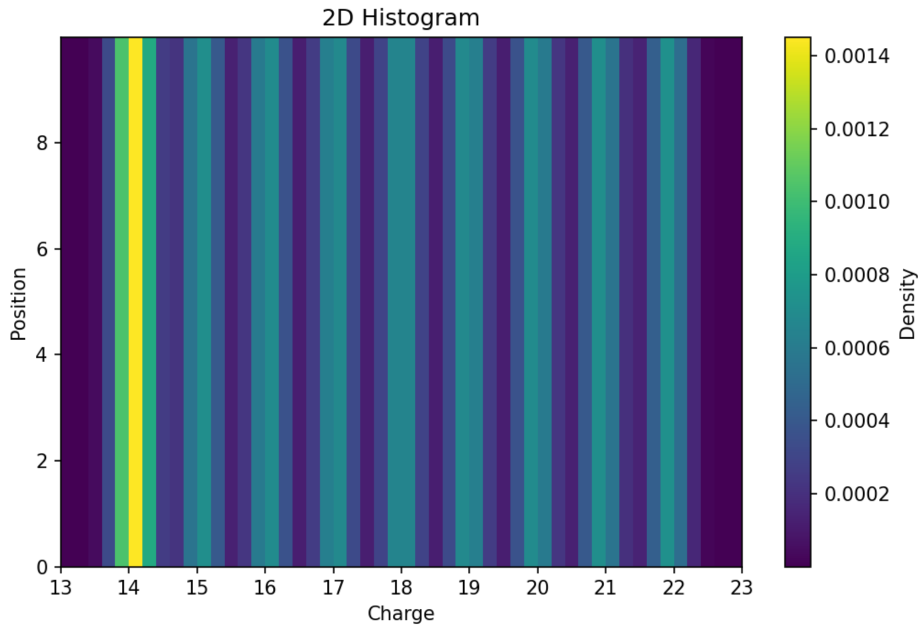

- Physics tells us that charge and position each follow specific distributions, and they are independent.
  - Hit position: Uniform distribution $U(x)$
  - Charge： Gaussian mixture distribution GMM(z)
- 2D distribution：

$$f(x,z)=U(x)\cdot \mathrm{GMM}(z)$$

- Method: build histograms of latent space distributions and use L1 constraint to match them with the physical prior distribution $f(x,z)$.

caveat：直方图不可导，无法直接用于反向传播，使用 Kernel Density Estimation (KDE) 来近似分布

Training Results

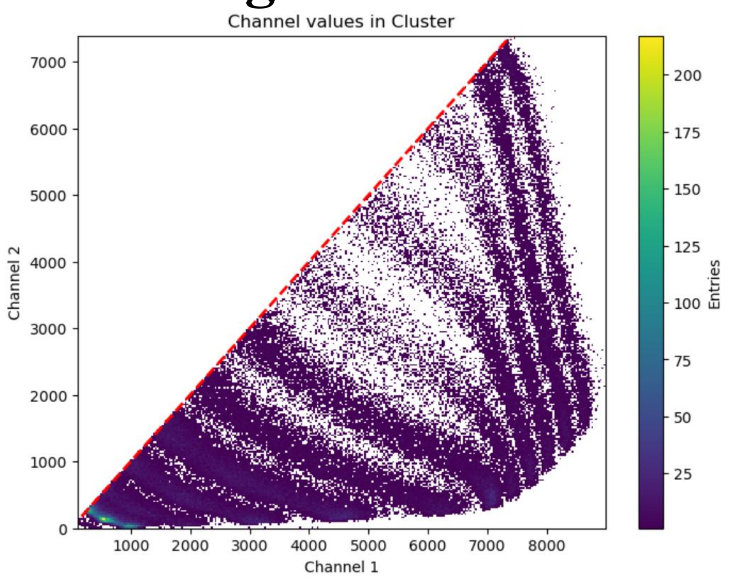

Input raw cluster

Encoder

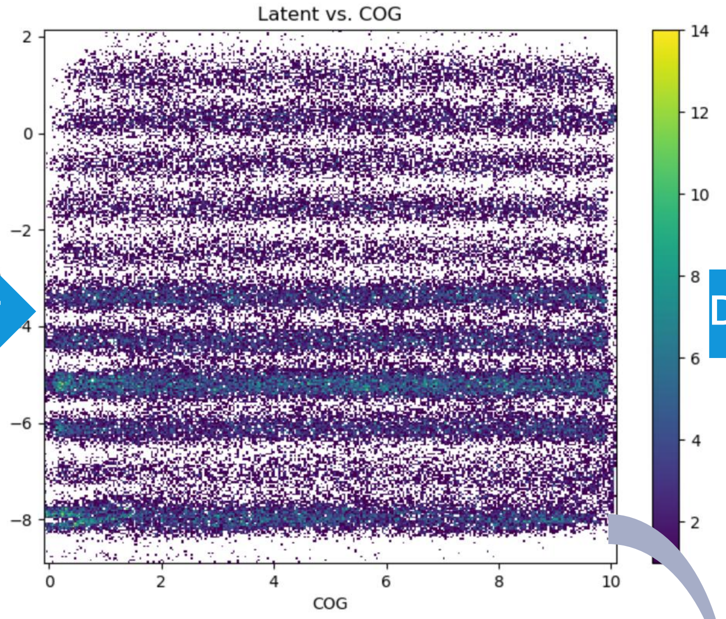

learnt latent space

Decoder

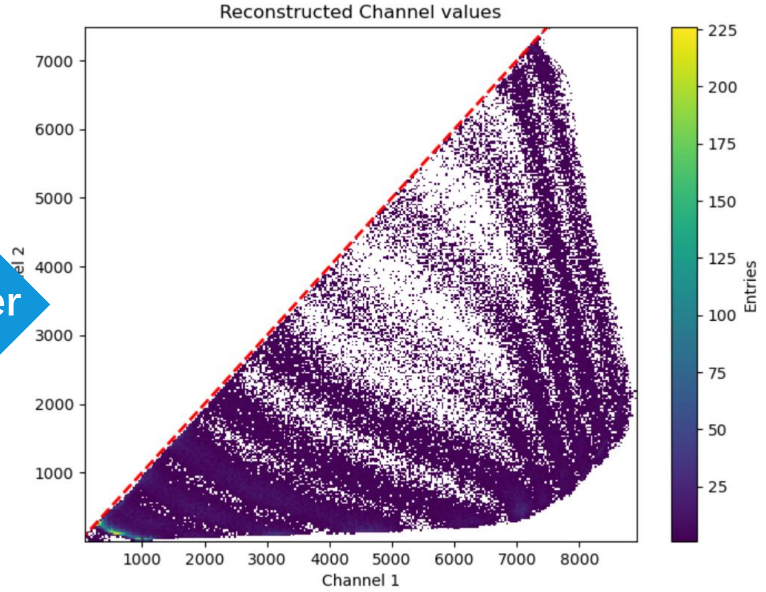

Reconstructed cluster

按truth电荷上色

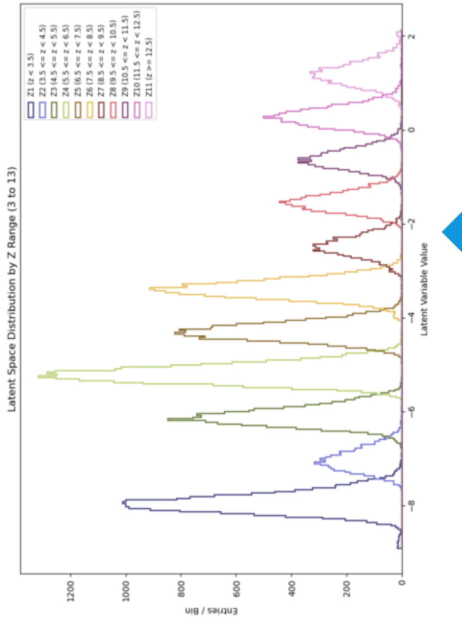

在z方向投影

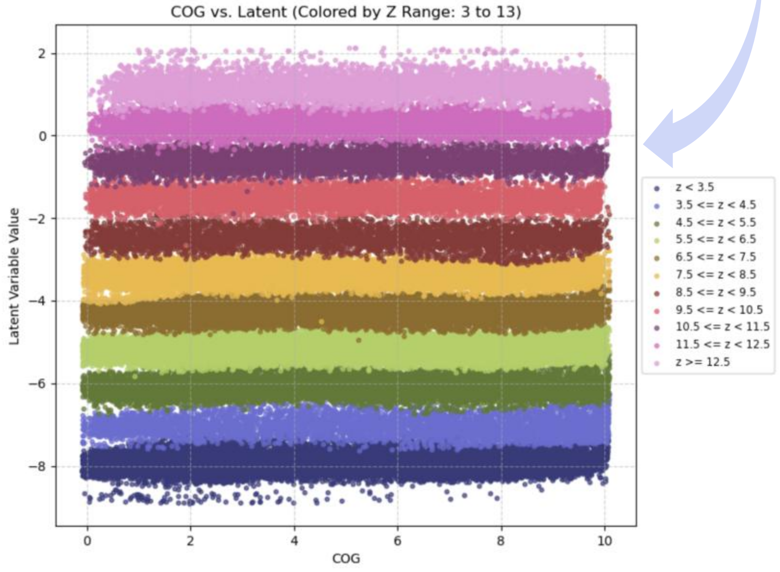

可见潜空间中每一个条带
对应了一种电荷的粒子

Charge/position measurement results

Latent space [0] distribution

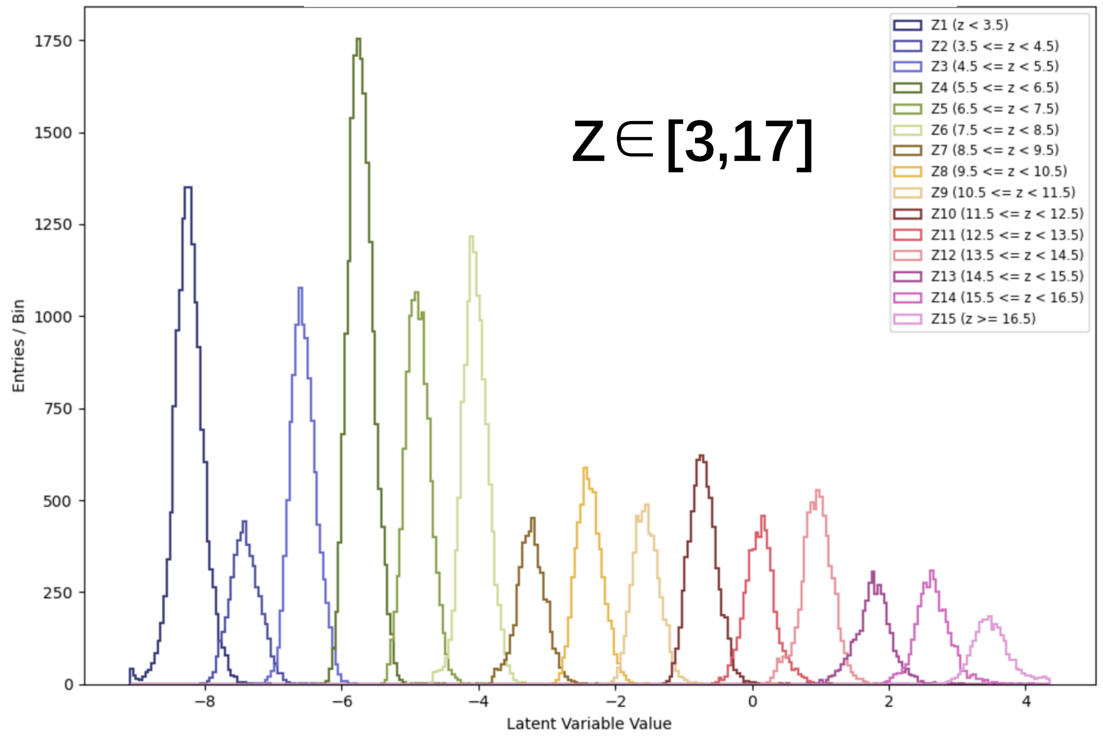

Latent space [1] vs COG

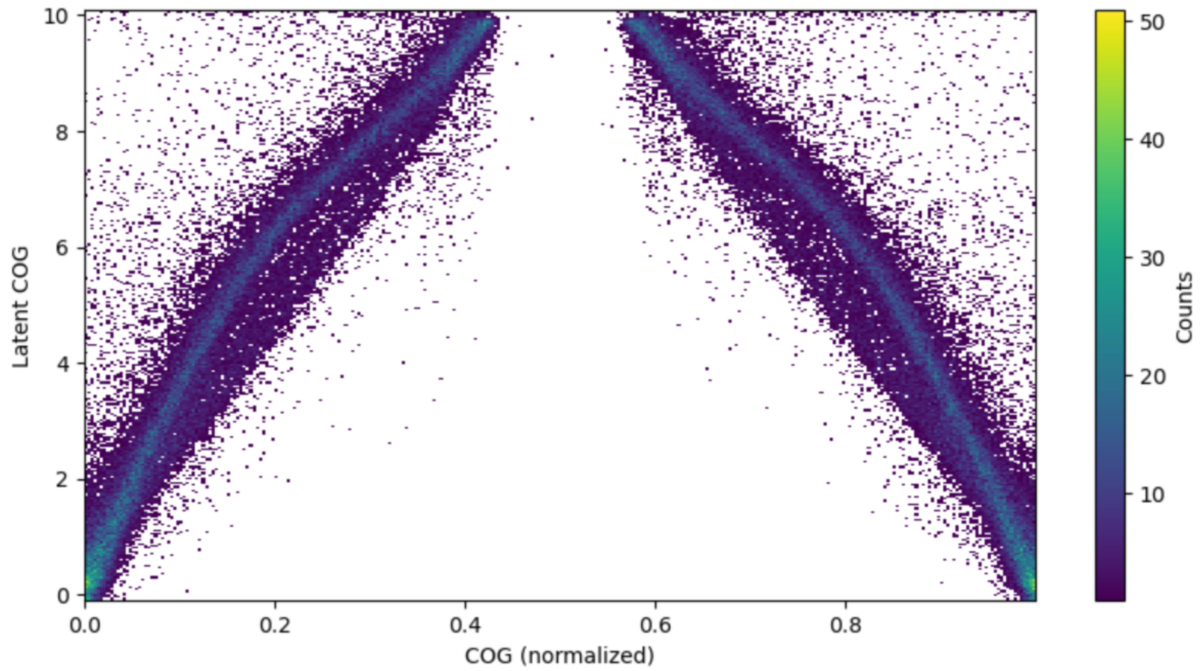

- Use truth information to indicate different colors
- Achievable up to Z = 22; higher Z requires larger statistics

- Latent space = 0 indicates a hit on a single strip; latent space = 10 indicates a hit between two strips

Paper draft preparing, to be submitted to EPJC/PRD [Corresponding author]

Proposal of measurement of nuclei fragmentation cross sections

Motivation

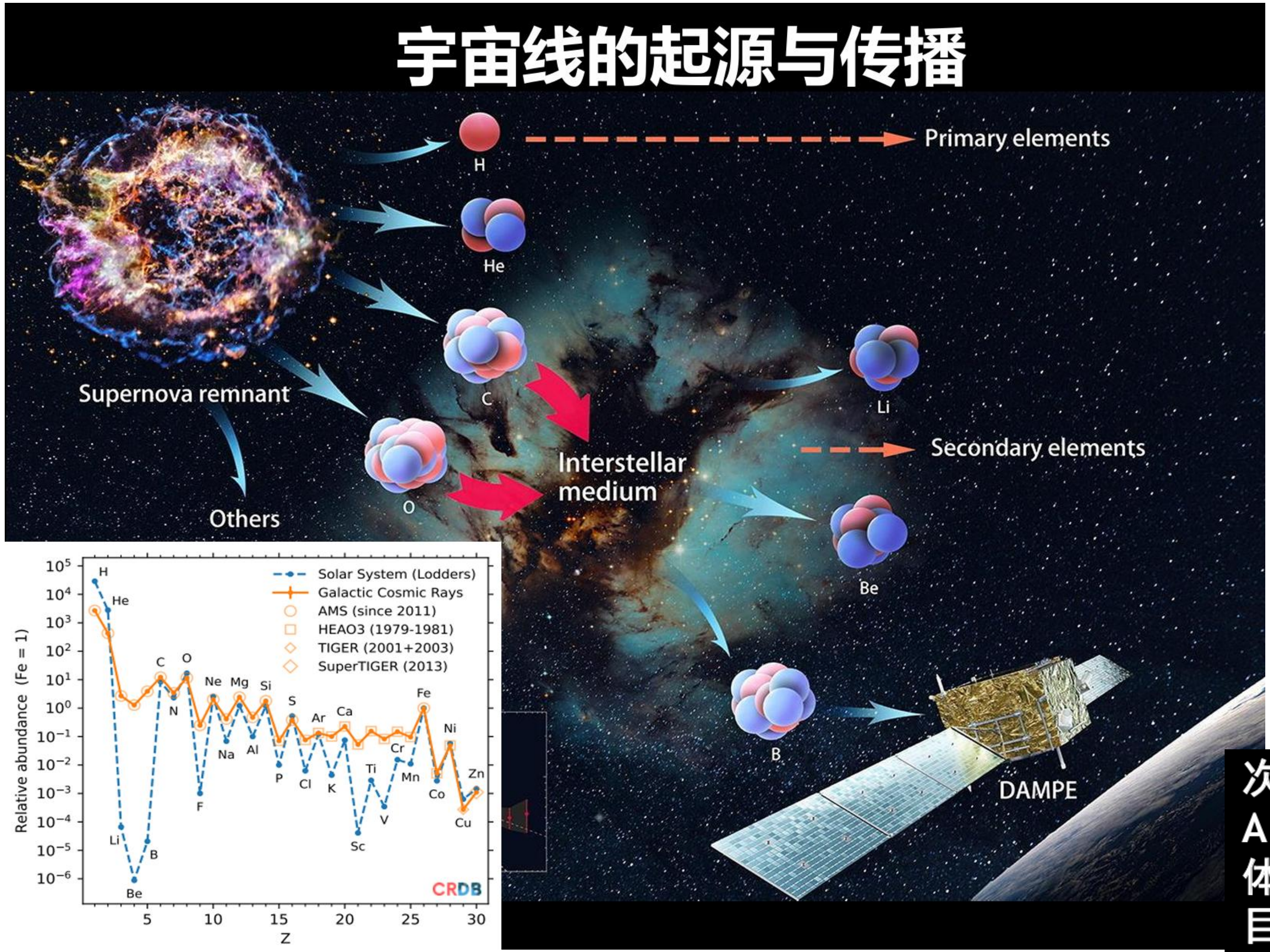

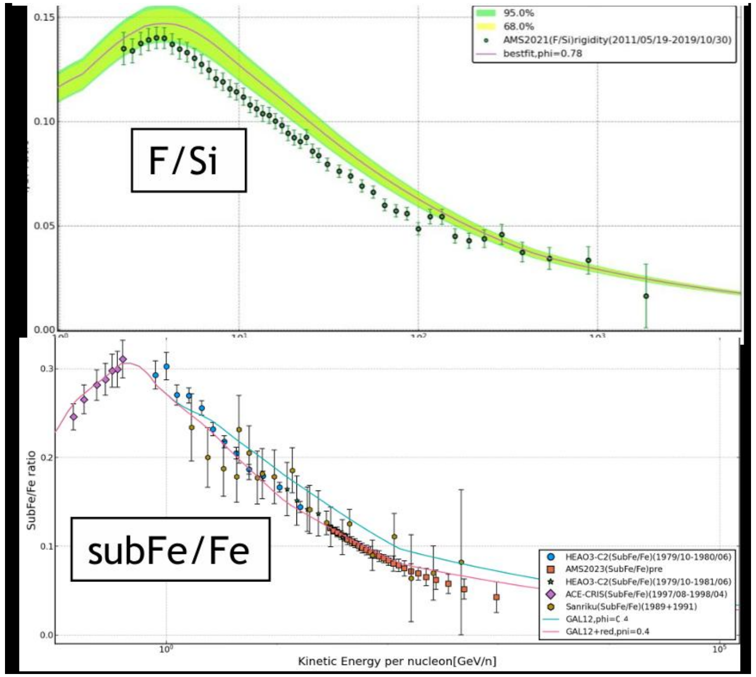

- Secondary cosmic rays are probes of the structure of the Galaxy

次级粒子的产生与什么有关？
A：1）银晕厚度和扩散系数。2）星际间介质气体密度。3）产生截面。
目前存在着一系列问题：Be/B比异常、Li异常、F高估，subFe/Fe可能也存在高估

Important channels to be measured

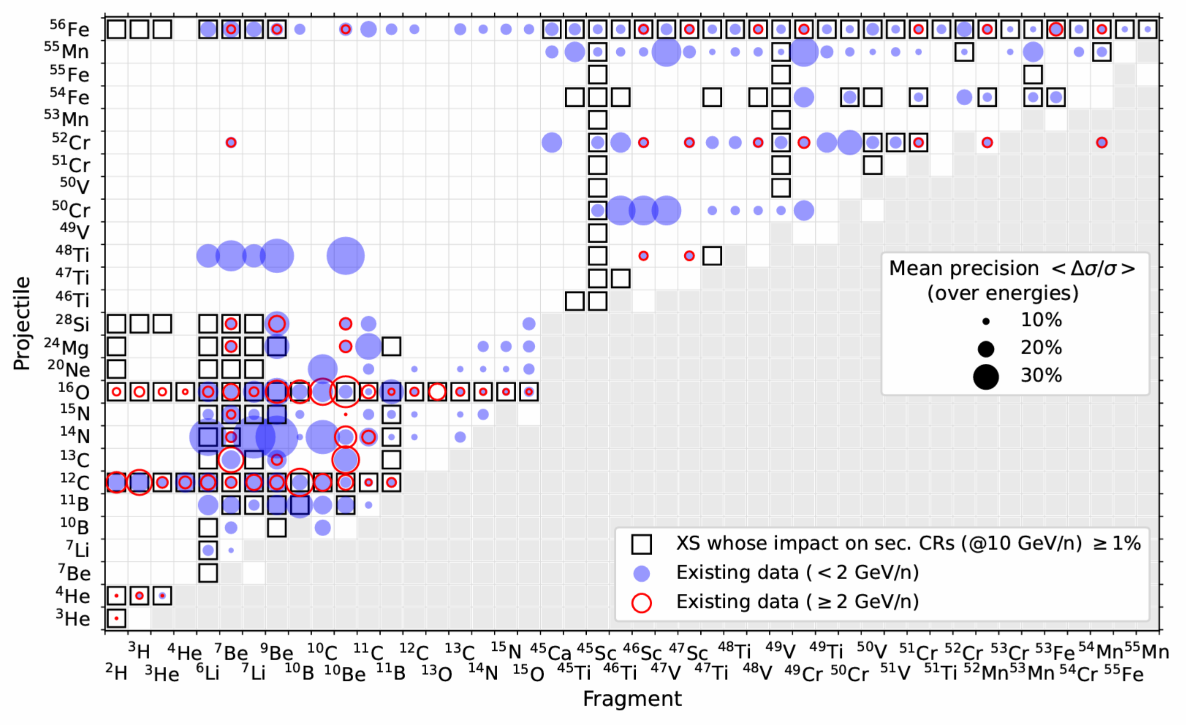

- C + H -> B/Li + X [double check NA61]
- O + H -> B/Li + X [high uncertain]

- Ne/Mg/N + H -> B/Li + X **[No measurement]**
- N + H -> B/Li + X **[No measurement]**

- C + C -> X

- X+ He -> X
- ……

Further Plan: HIAF and CERN

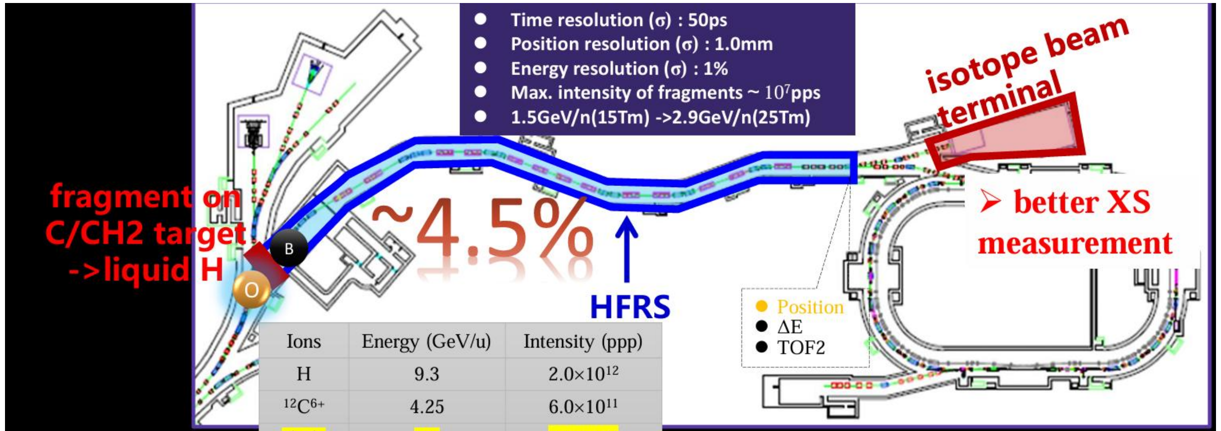

Ions	Energy (GeV/u)	Intensity (ppp)
H	9.3	2.0×10^{12}
$^{12}C^{6+}$	4.25	6.0×10^{11}
$^{16}O^{6+}$	3.0	4.0×10^{11}
$^{36}Ar^{12+}$	2.6	2×10^{11}
$^{58}Ni^{18+}$	2.37	1.4×10^{11}
$^{78}Kr^{19+}$	1.72	1.2×10^{11}

Parameters of HFRS compared with others

	Length (m)	Beam size at target (mm)	Angular acceptance(mrad)	Momentum acceptance (%)	Resolving power	Max. Bρ (Tm)
HFRS NIM.B 547(2024),165214	191.38	±1/±1.5	±30 (X); ±25 (Y)	±2.0	850/1100 (ΔX=±1mm)	15->25
SuperFRS NIM.B 204(2003),71	182.2	±1/±2	±40 (X); ±20 (Y)	±2.5	750/1500 (ΔX=±1mm)	20
BigRIPS Prog.Theor.EXP.Phys.2012,03 C003	78.2	±0.5/±0.5	±40 (X); ±50 (Y)	±3	1260/3420 (ΔX=±0.5mm)	9.5
ARIS NIM.B 317(2013), 349	86.8	±0.5/±0.5	±40 (X); ±40 (Y)	±5	1720/3000 (ΔX=±0.5mm)	8

@SPS H4 2024.11

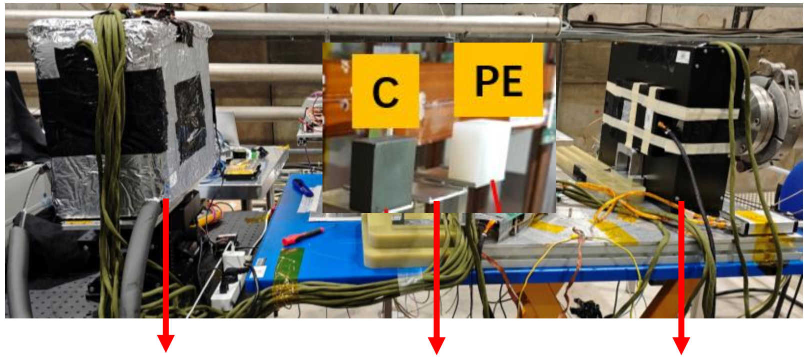

- Combined with TOF, for isotope identification => LGAD, TPC?

Summary

- AMS L0 Tracker upgrade detector construction, QC, and space qualification
- Silicon strip detector performance study
- Double-η algorithm for position reconstruction and BDT/ML algorithm for PID
- Proposal of nuclei fragmentation XS measurement @HIAF and CERN

Thanks!

Backup

The AM

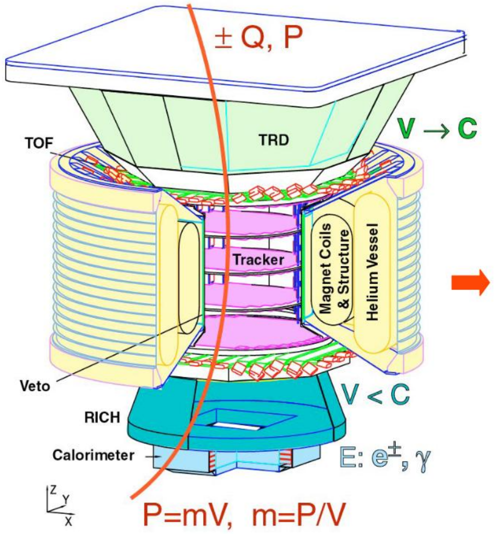

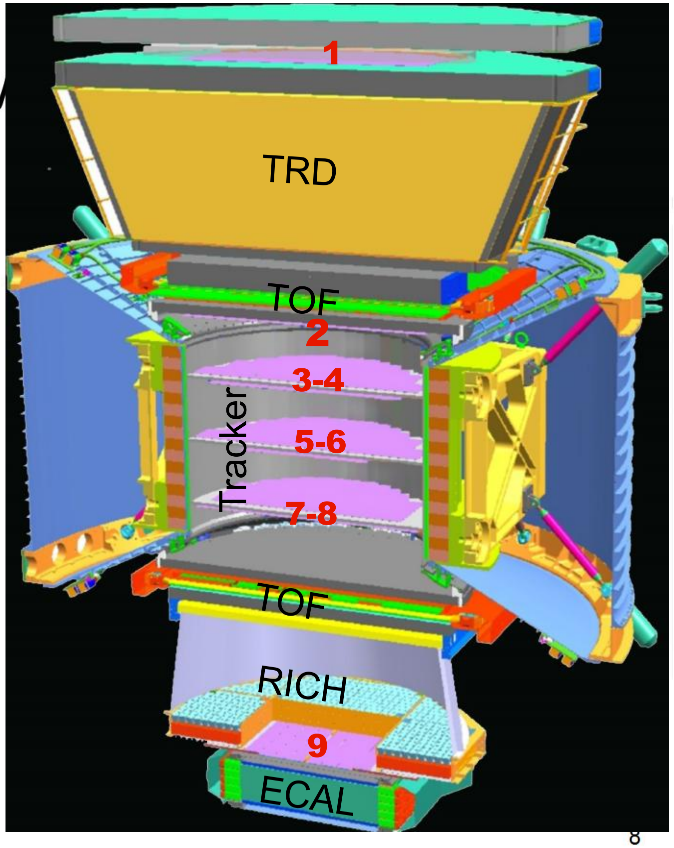

Superconducting magnet

- 2 'dipole' coil, 12 'racetrack' coil (~ no magnetic dipole moment)
- B~0.9 T, 1.1 m inner diameter, 2360 Kg weight
- 55 Km of superconducting wire (NbTi/Cu embedded in pure aluminium)
- Indirect cooling with superfluid helium (1.8 K)
- 2500 liters helium vessel plus cryocuulers for 3 years operation

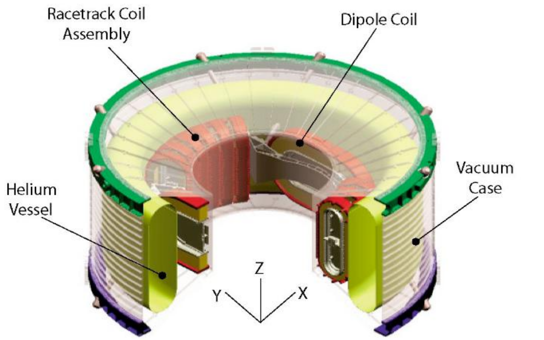

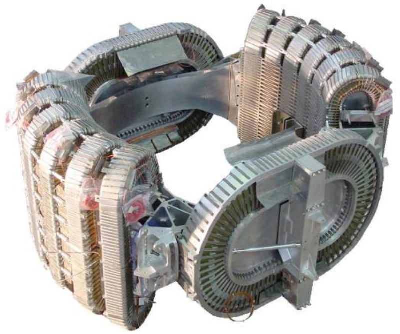

- AMS02: 0.15 T

Tracker P-Side Hybrids

VA_hdr

capacitor chip

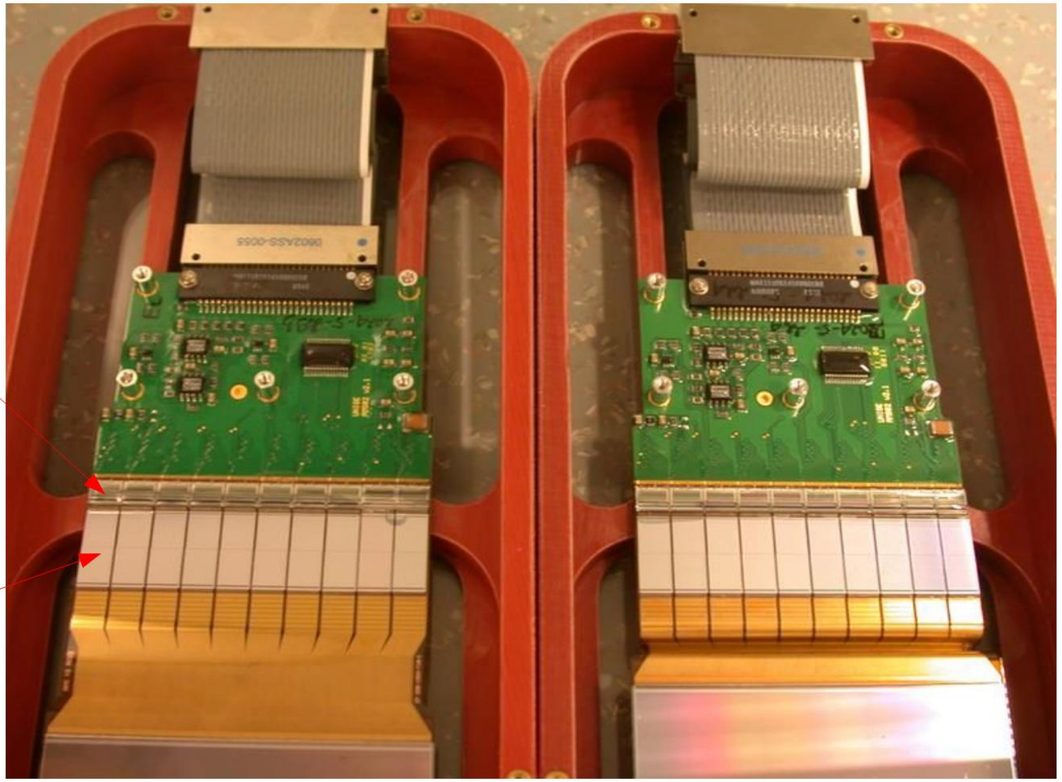

AMS-02 Silicon Detectors

- sensor dimensions: 4.136 x 7.205 x 0.03 cm^3
- n-type silicon with implantation/readout strip pitches
  p-side: 27.5/110 microns, type p^+
  n-side: 52.0/208 microns, types n^+ and p^+ blocking
- capacitive charge coupling
  p-side: 3 floating strips
  n-side: 1 floating and 2 blocking strips

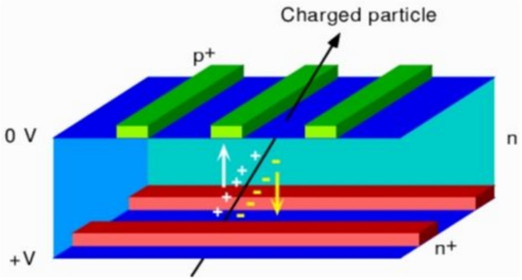

p^+ blocking strips not shown

QM平面整体集成 – Ladder安装

中国科学院高能物理研究所
Institute of High Energy Physics Chinese Academy of Sciences

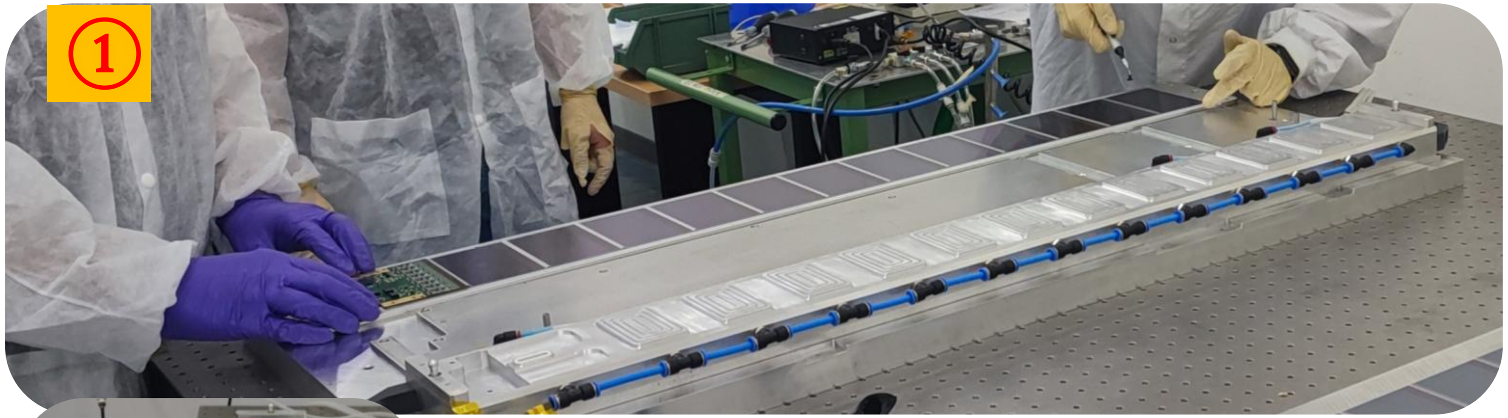

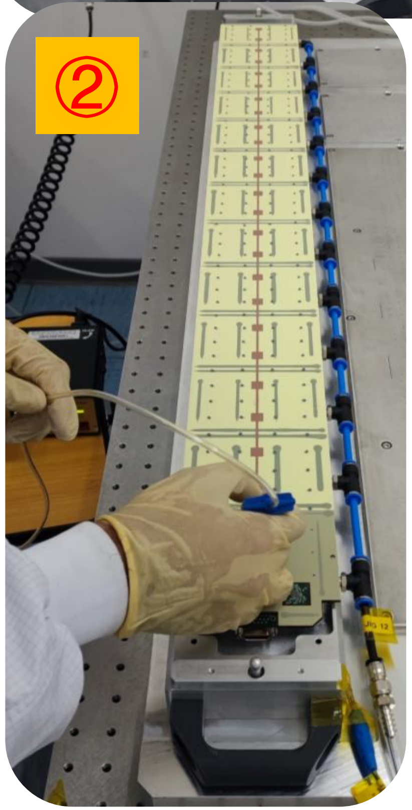

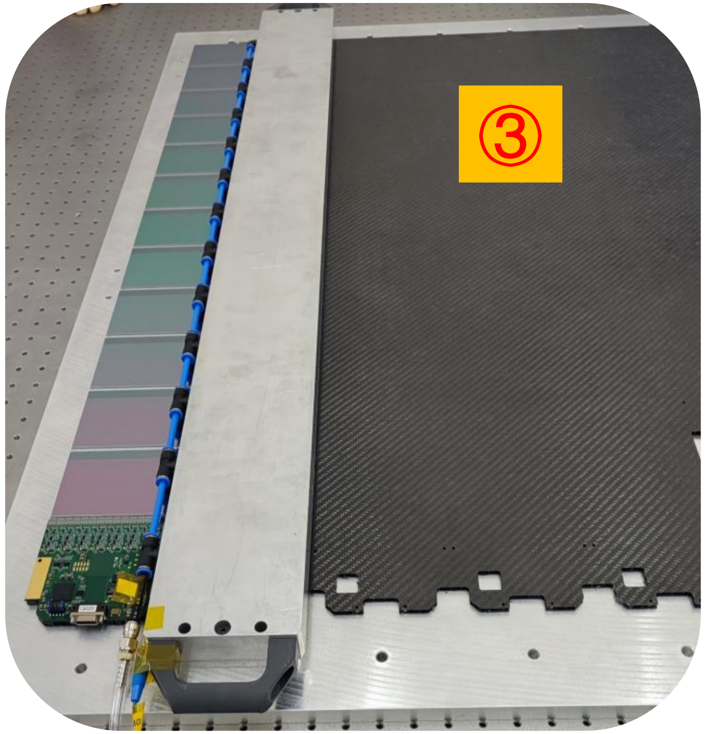

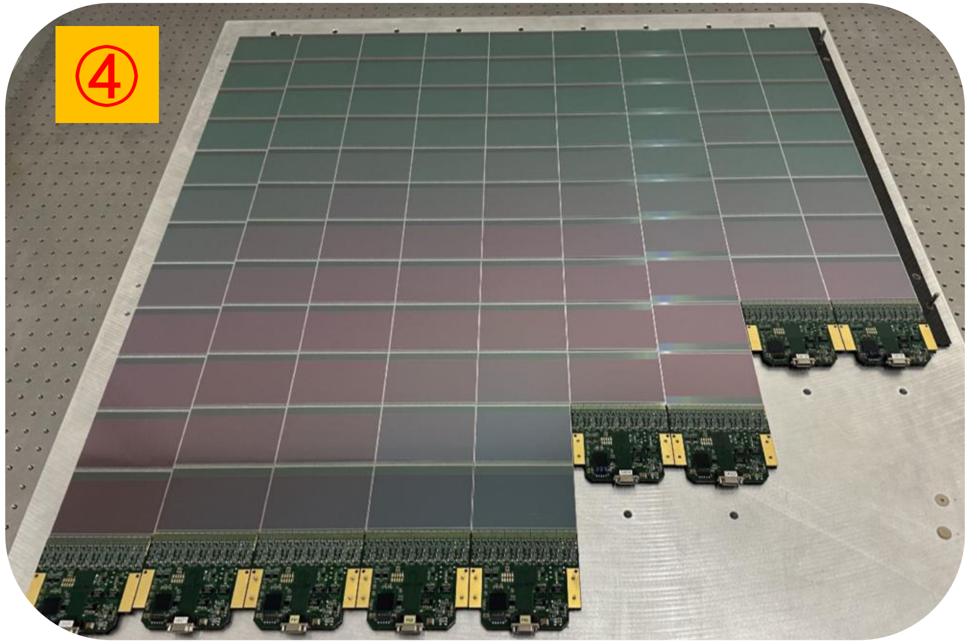

- 使用结构胶将Ladder固定在碳纤维支撑(QLCS)上

Beam data analysis process

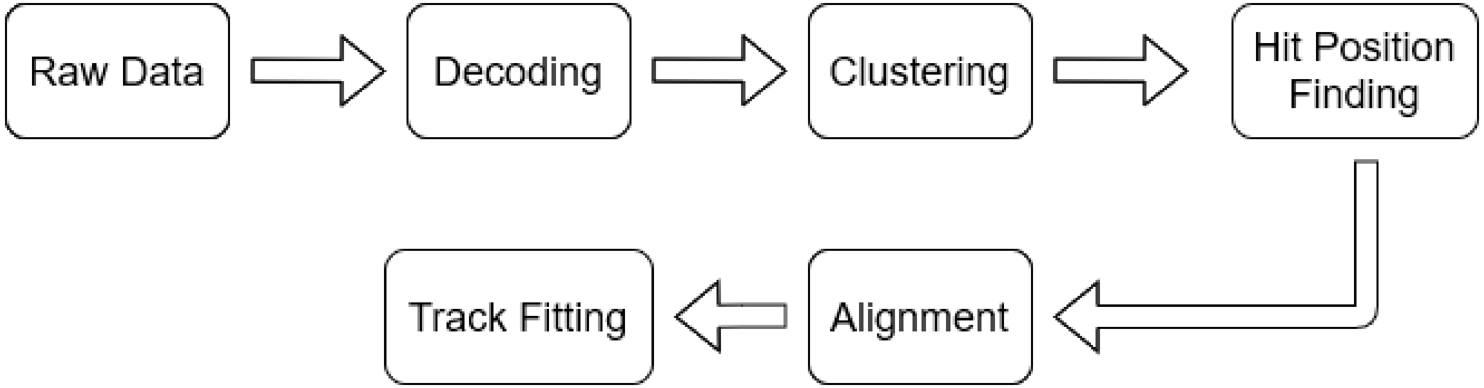

- Decode ADC value from binary raw data
- Form clustering hits after pedestal and common noise subtraction
- Reconstruct 3-D tracks for DUT performance study
- Use MILLEPEDE-II method for solution of detector alignment and GeneralBrokenLines(GBL) algorithm for track fitting
- Develop a non-linear eta algorithm for hit position reconstruction

Millepede-II V04-16-00

Hit position reconstruction => double-η

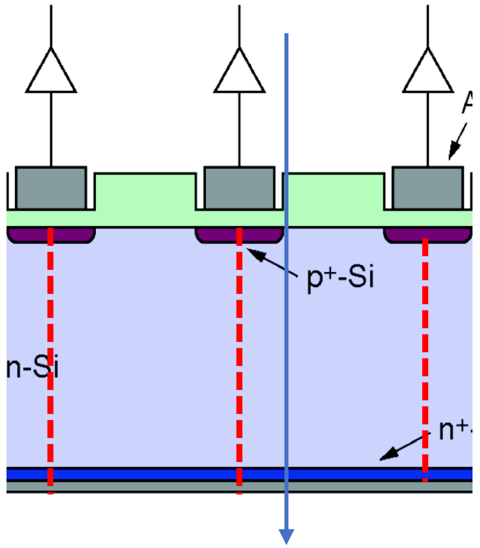

$$X_{COG} = \sum_{cluster} S_i x_i \Big/ \sum_{cluster} S_i ,$$

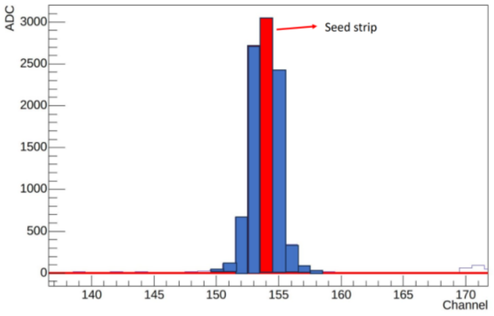

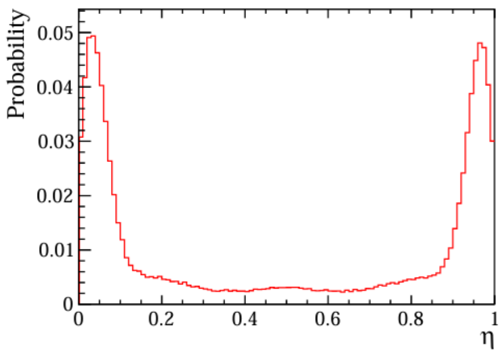

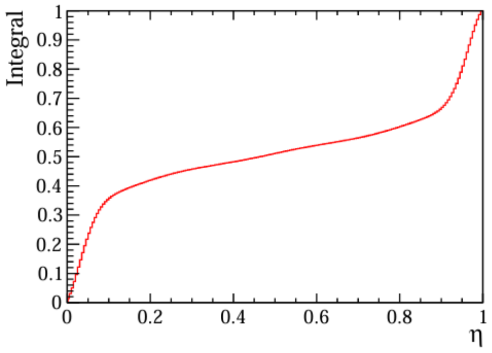

$$\eta = \frac{S_R}{S_R + S_L},$$

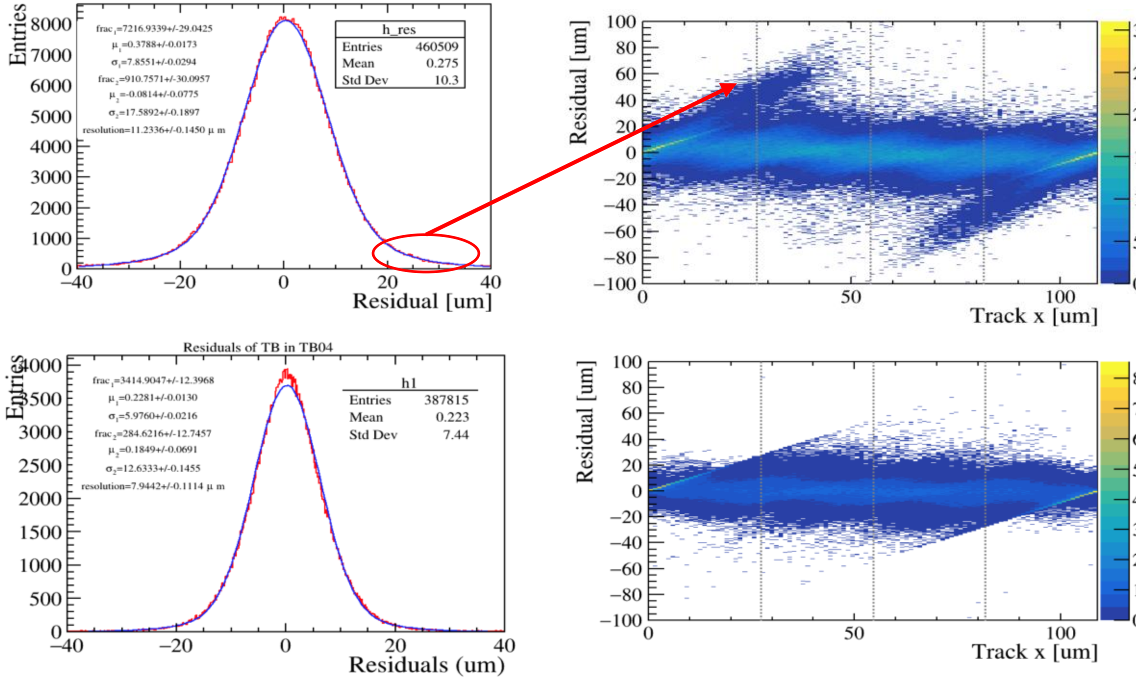

- Charge sharing between strips is nonlinear, the eta algorithm can reflect this nonlinearity [Nucl.Instrum.Meth.A 335 (1993) 44-58]
- When the detector noise causes the signal size to flip, there will be a large deviation

Preamplifier study by charge injection

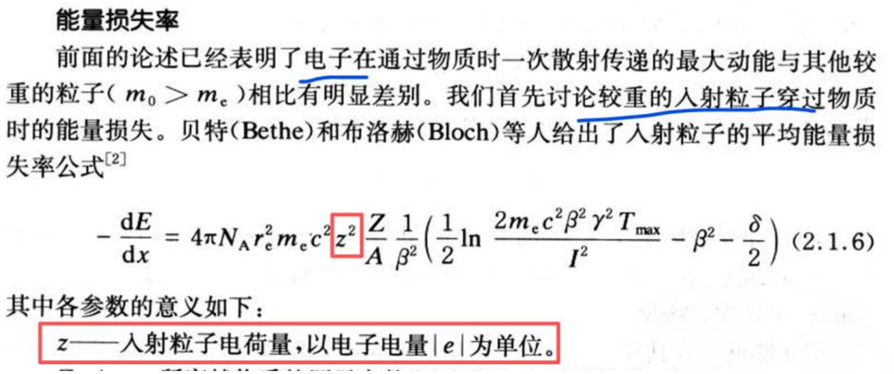

能量损失率

前面的论述已经表明了电子在通过物质时一次散射传递的最大动能与其他较重的粒子($m_0 > m_e$)相比有明显差别。我们首先讨论较重的入射粒子穿过物质时的能量损失。贝特(Bethe)和布洛赫(Bloch)等人给出了入射粒子的平均能量损失率公式[2]

$$-\frac{dE}{dx} = 4\pi N_A r_e^2 m_e c^2 z^2 \frac{Z}{A}\frac{1}{\beta^2}\left(\frac{1}{2}\ln\frac{2m_e c^2\beta^2\gamma^2 T_{max}}{I^2} - \beta^2 - \frac{\delta}{2}\right) \quad (2.1.6)$$

其中各参数的意义如下：

z——入射粒子电荷量，以电子电量|e|为单位。

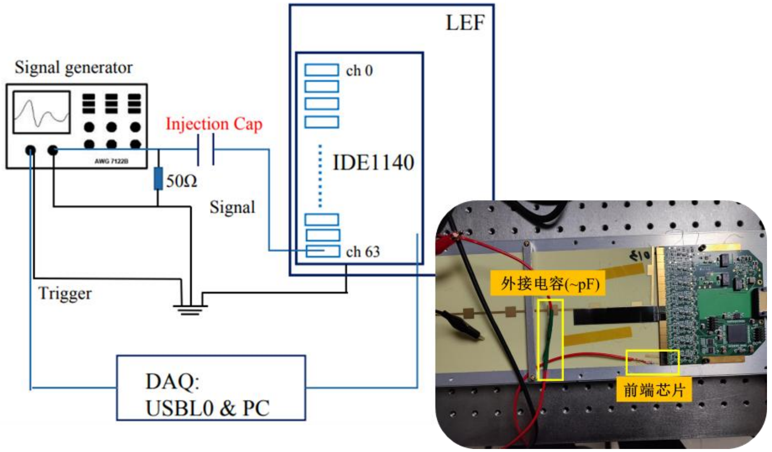

- For MIPs with Z=1, the electron-hole pairs generated through 300um thick silicon are 4fC
  - For an iron (Z=26), the charge is 2700 fC
- Studying the saturation (dynamic range) of preamplifier using charge injection
  - Optimization of feedback resistance
- Bilinear dynamic range, up to Z=22
  - Charge sharing enhances PID performance

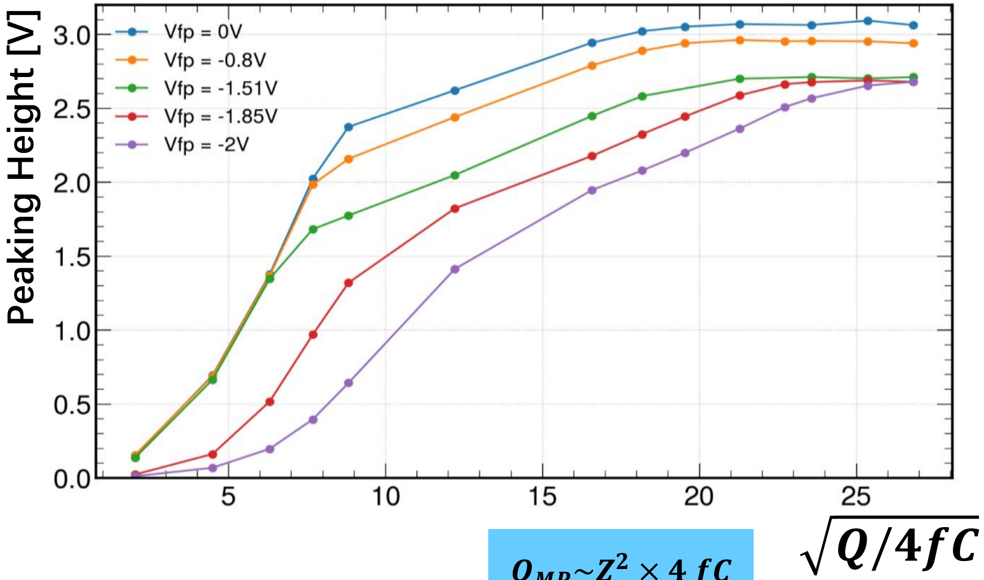

$Q_{MP} \sim Z^2 \times 4\,fC$

AMS-02 Heavy nuclei PID algorithm

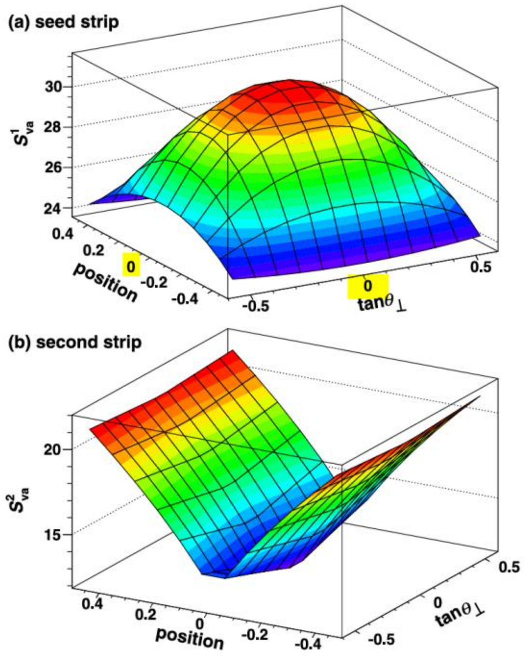

Fig. 6. Position and $\tan\theta_\perp$ dependence of the y-side signal with a silicon nuclei sample for the (a) seed strip and (b) second strip.

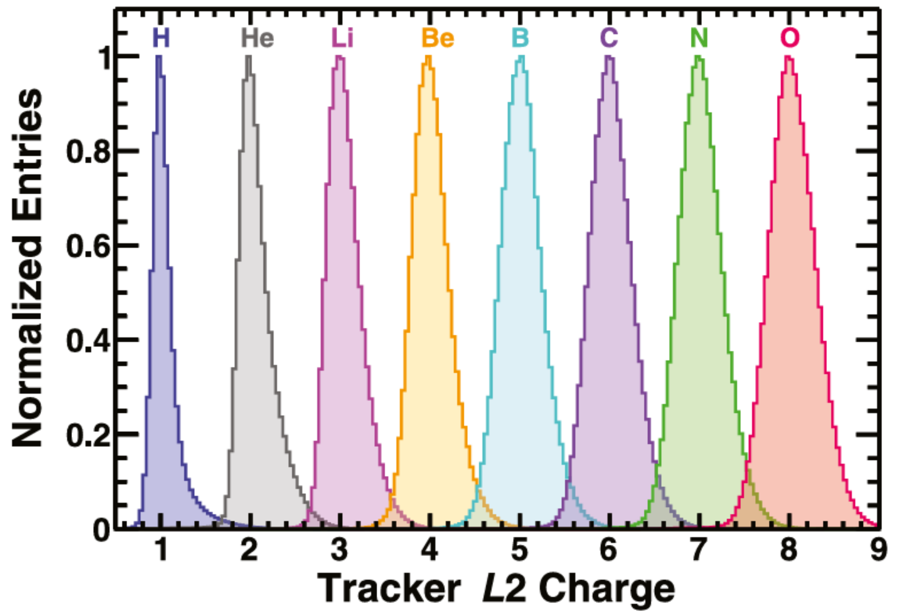

Fig. 12. The charge distribution on tracker $L2$ for $1 \leq Z \leq 8$ selected by the TOF, tracker $L1$, and tracker $L3$-$L8$ with rigidity > 7 GV. The peak value of each species is normalized to 1.

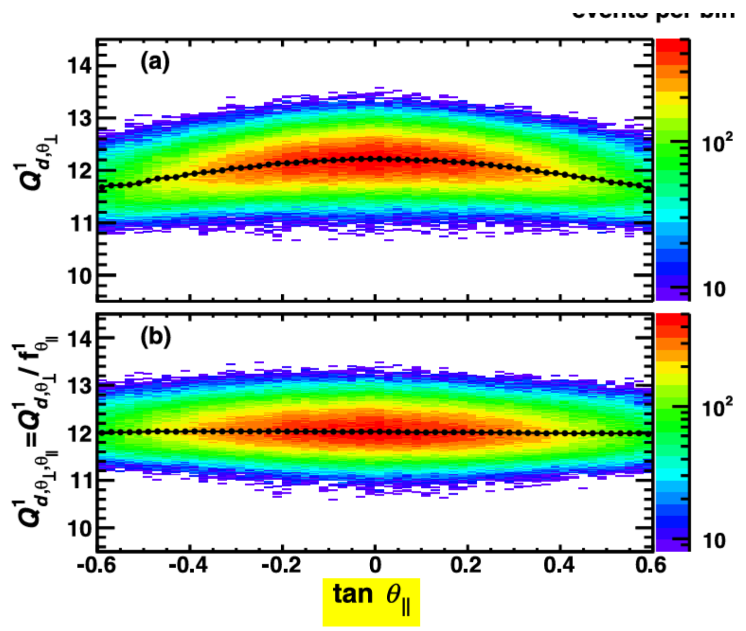

Fig. 7. The magnesium signal distribution of the y-seed seed strip on tracker $L5$ as a function of $\tan\theta_\parallel$ (a) before and (b) after applying $f^1_{\theta_\parallel}$.

Comparison with related work

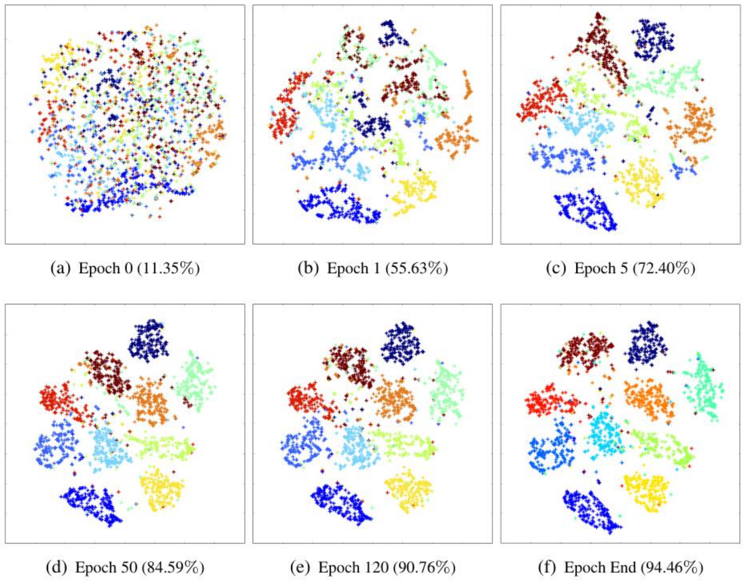

Figure 3: The illustration about how data is clustered in the latent space learned by VaDE during training on MNIST. Different colors indicate different ground-truth classes and the clustering accuracy at the corresponding epoch is reported in the bracket. It is clear to see that the latent representations become more and more suitable for clustering during training, which can also be proved by the increasing clustering accuracy.

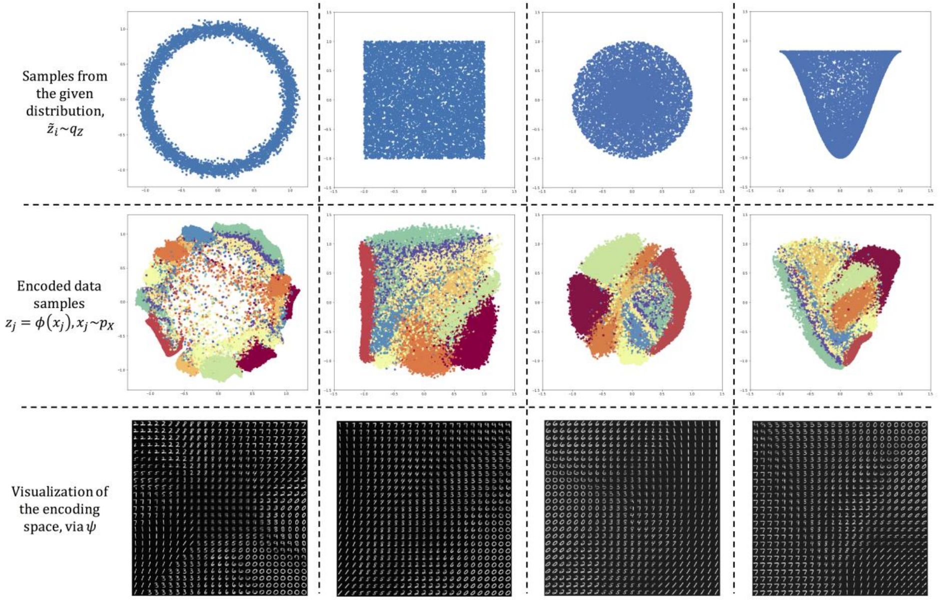

Figure 3: The results of SWAE on the MNIST dataset with a two-dimensional embedding space for four different distributions as ,q_Z, namely the ring distribution (top left), the uniform distribution (bottom left), the uniform polar distribution (top right), and a custom polar distribution (bottom right). Note that the far right visualization demonstrates the decoding of a 25×25 grid in $[-1, 1]^2$.

Achieved classification of diverse objects, but latent space geometry remains uncontrolled [IJCAI 2017]

Can control the overall latent space geometry, but not its internal fine structure [ICLR2019]

表面静电荷对噪声影响

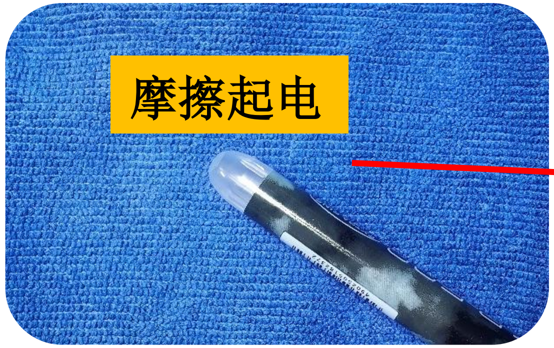

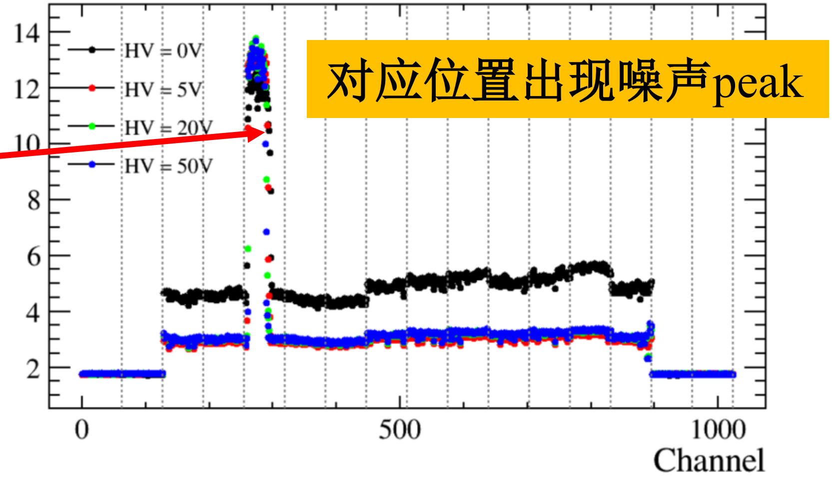

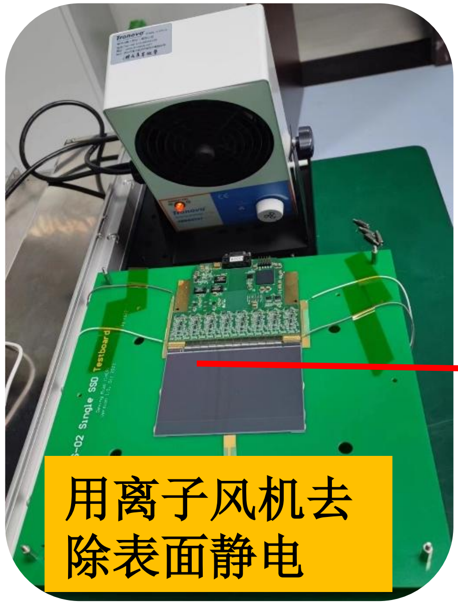

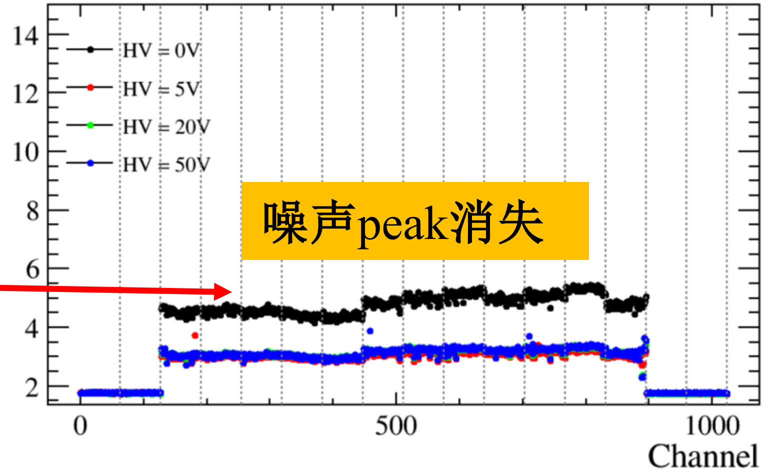

- 确认噪声来源是sensor表面静电荷，并且可以去除
- 在后续生产中进行工件的防静电处理(接地，离子风机除静电)
- 目前8+1个探测器都可以正常工作

[1] study is inspired by ATLAS ITK detector: Nuclear Inst. and Methods in Physics Research, A 978 (2020) 16440

AMS L0的束流测试

研究目标

- 搭建Beam Monitor, 验证其位置分辨率 **[done]**
- Bias resistor区域的探测效率研究 **[done]**
- 研究重核在探测器中的响应
  - 重核PID，重核位置分辨 **[done]**
  - 重核斜入射的重建算法研究 **[on going]**
- 探测器升空前的束流校准

几次束流测试

- 2023年 8月，@SPS, p(180GeV) & μ^-
- 2023年10月，@SPS, 混合重核束流
- 2024年 1月，@BSRF, 低能电子束流
- 2024年 5月，@SPS, 缪子束流
- 2024年11月，@SPS, 混合重核束流，与HERD联合取数

重核斜入射研究setup

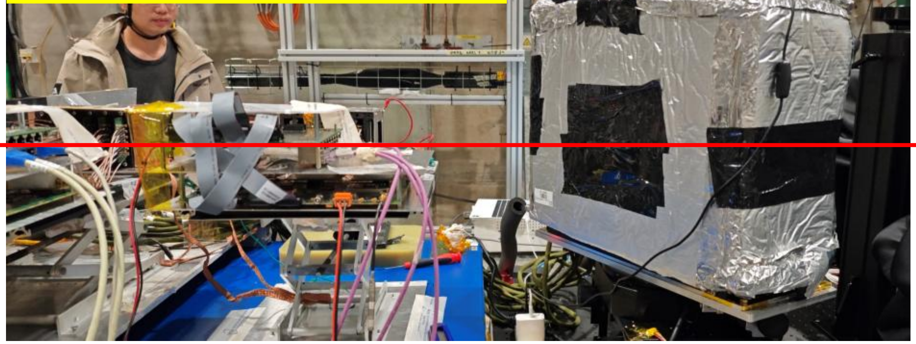

@SPS H4 2024.11, 与帮我搭探测器的兄弟们

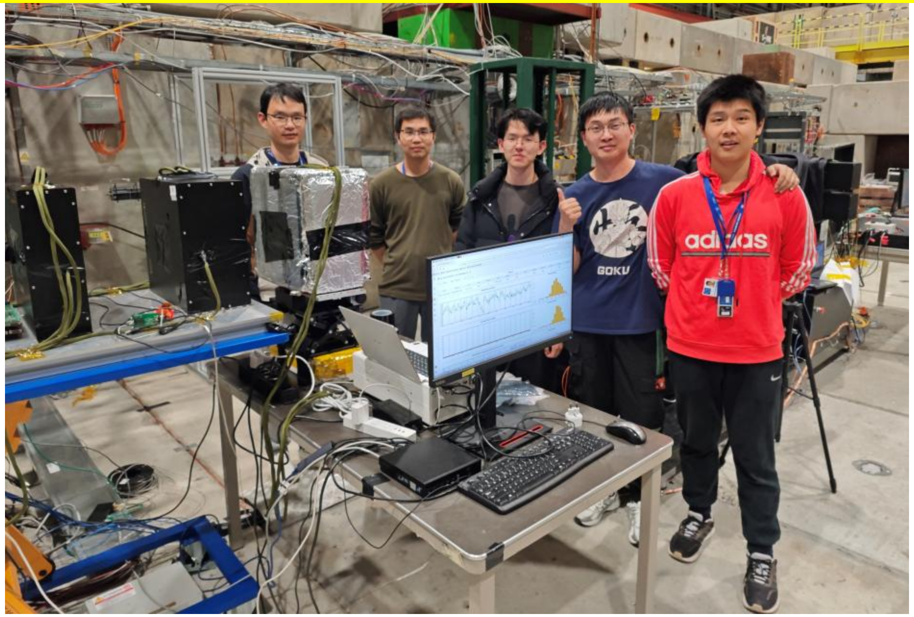

AMS L0与HERD的联合探测器研究

研究目标

- 利用我们自己搭建的**Beam Monitor**, 给HERD各子探测器提供径迹信息，进行探测器刻度与性能研究
- 对AML0 Ladder本身对MIP的性能进行详细研究
- 研究AMSL0 SSD共同流片baby sensor对MIP的性能与优化

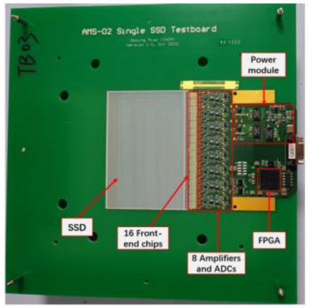

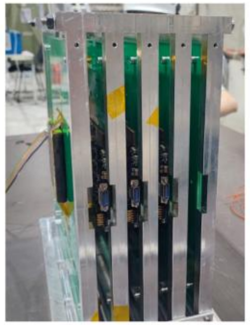

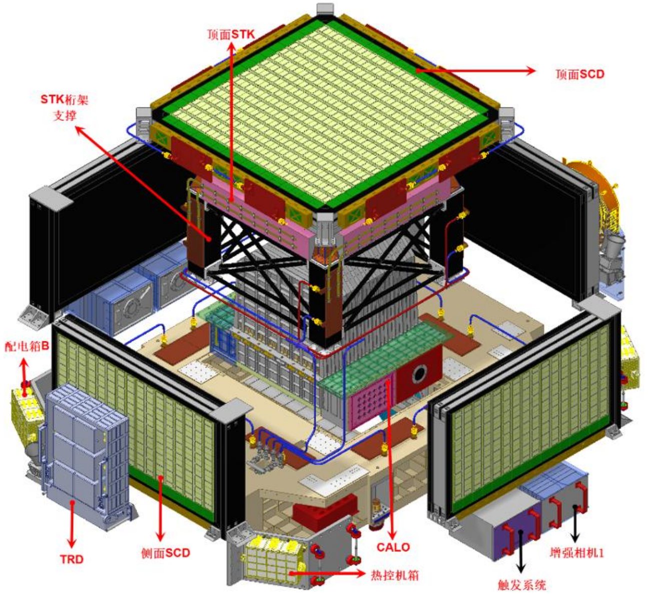

多次联合测试

- 2024年11月，@SPS, 混合重核束流
- **2025年6月，@IHEP，与STK联合取宇宙线**
- **2025年7月31-8月6号，@SPS，高能质子与电子束流测试**
- **2025年8月11-9月3号，@PS，低能质子/电子/pion束流测试**

Plasma Effect of High-energy Heavy Nuclei

Plasma delay effect in silicon detector

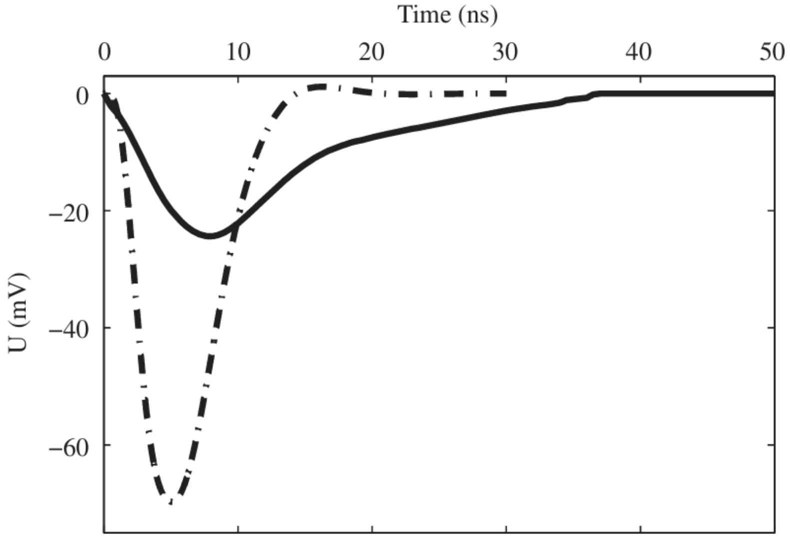

Fig. 1. Mean experimental current signal induced by 80 MeV ^{12}C ions impinging on the rear side of a silicon detector [3]—full line; the simulation using undisturbed electric field—dashed-dotted line—completely fails.

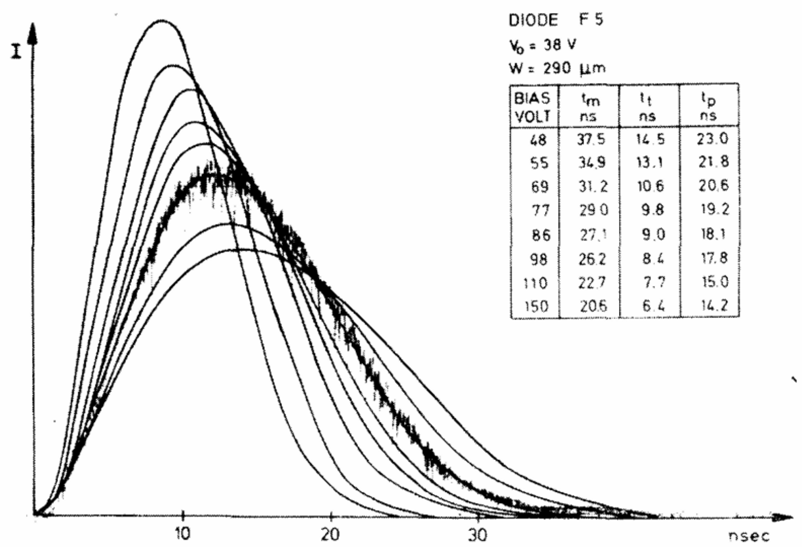

BIAS VOLT	t_m ns	t_t ns	t_p ns
48	37.5	14.5	23.0
55	34.9	13.1	21.8
69	31.2	10.6	20.6
77	29.0	9.8	19.2
86	27.1	9.0	18.1
98	26.2	8.4	17.8
110	22.7	7.7	15.0
150	20.6	6.4	14.2

Fig. 4. Current pulse shapes obtained with detector F5, for front-injected 42 MeV ^{16}O ions, at different bias voltages.

- Observed in low-energy nuclear physics experiments
  - The rising edge speed of heavy nucleus signals is significantly slower
  - Increasing the reverse bias voltage can make the rising edge faster
- This is explained by the damage caused by a huge electron-hole pairs (plasma) to **disturbed (shield)** the built-in electric field of silicon

Shift effect of heavy nuclei tracking

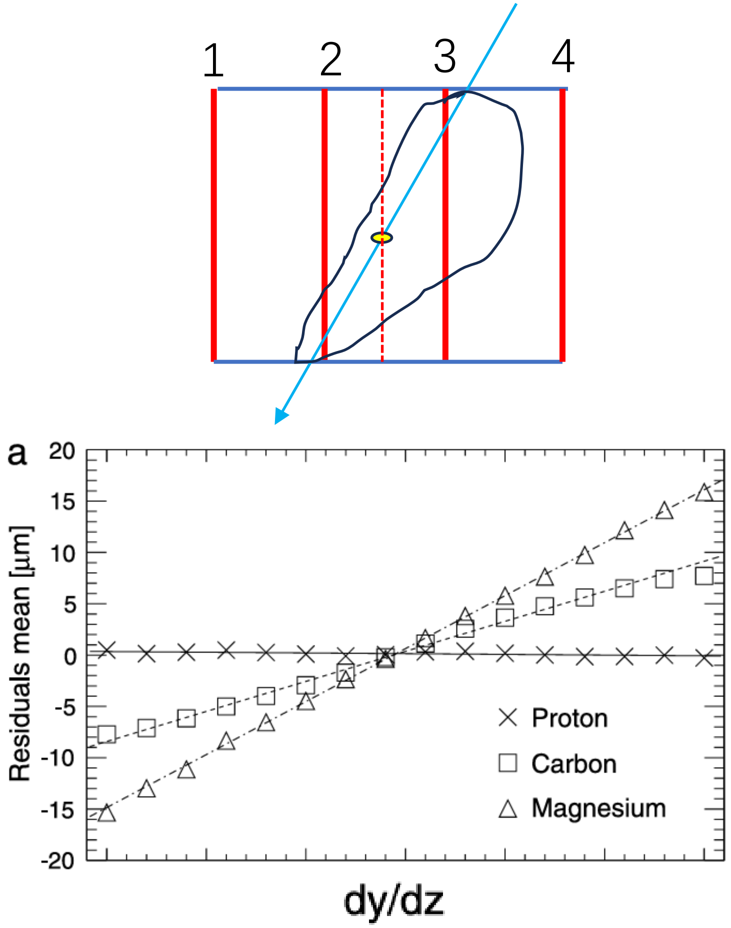

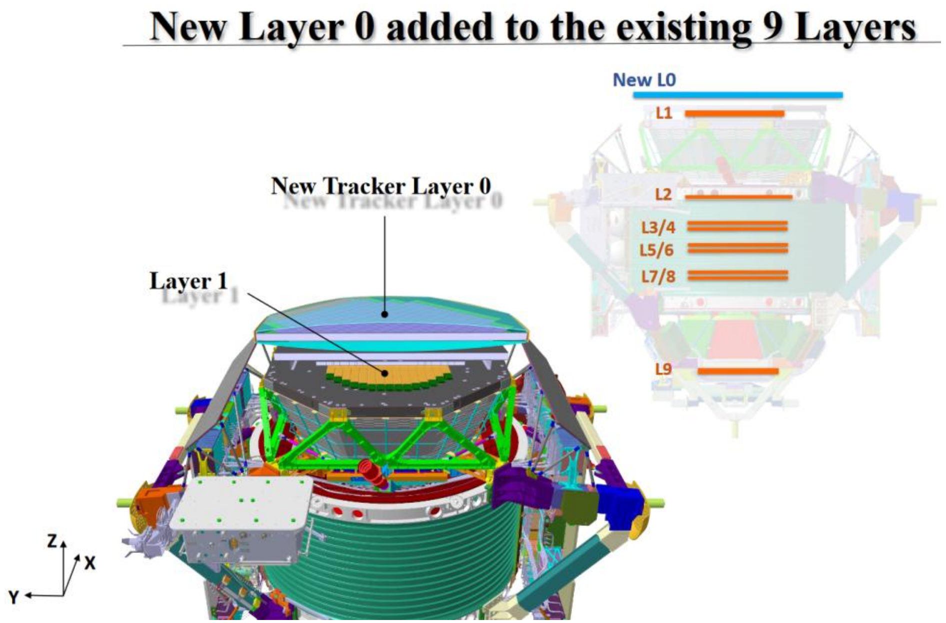

- The position reconstruction of incident particles will be affected by the plasma effect => 近大远小
- AMS02 observed this phenomenon while in orbit NIMA 869 (2017) 29–3
- L0 is far away from other trackers, so this effect needs to be measured on the ground in advance
- Better understanding of the plasma effect through simulation

Beam test Setup

整体旋转，相当于斜入射

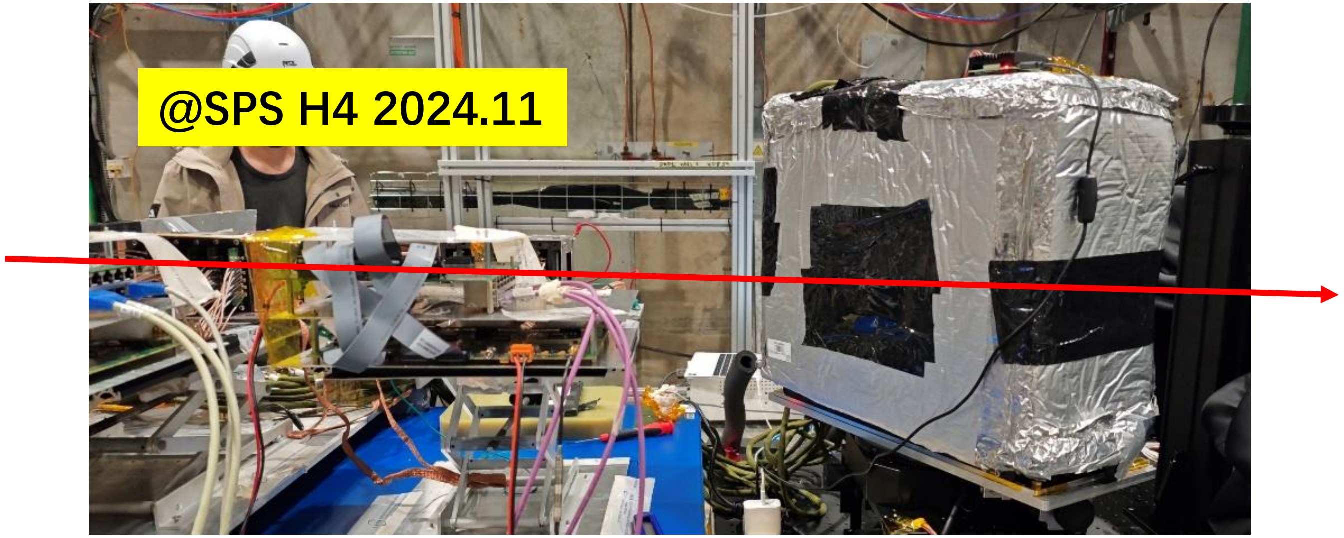

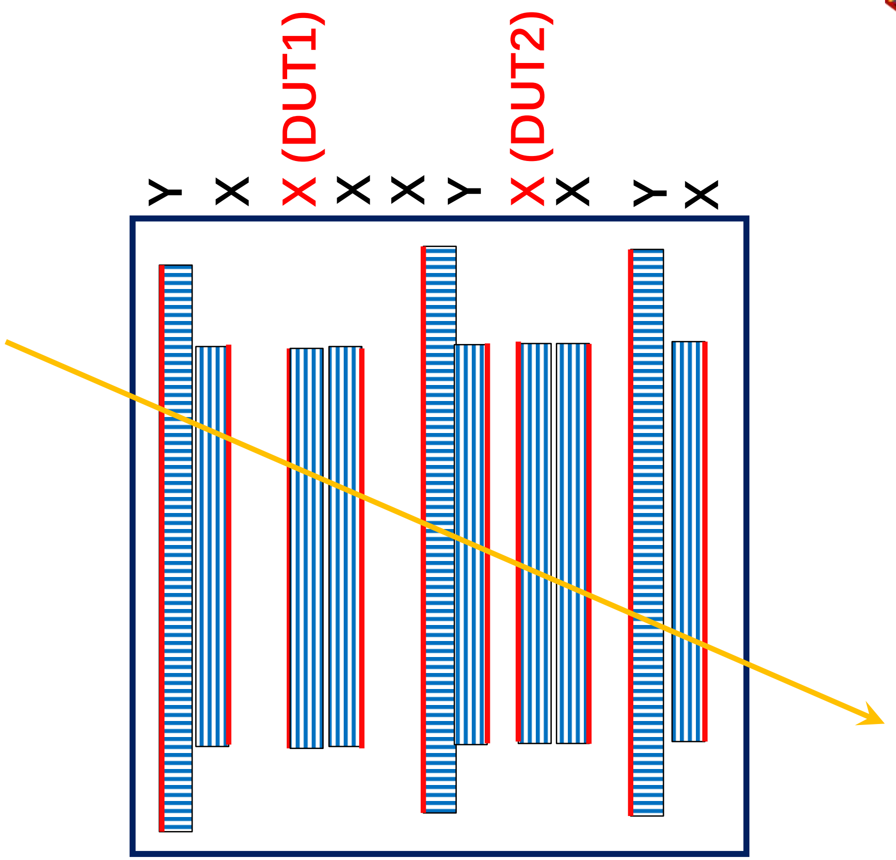

- Rotate the entire telescope **along the y-axis** to different angles
- 5 x-layers are back to the beam, and 2 x-layers are facing the beam
  - The shift reconstructed position is in the opposite direction
  - Using the back-layers reconstructed track to measure the facing deviation, can get double shift

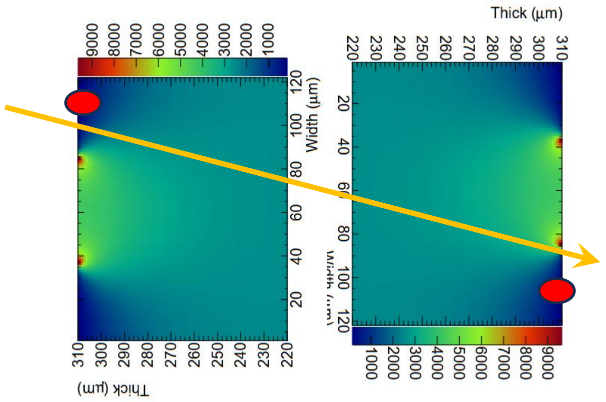

Measured shift value

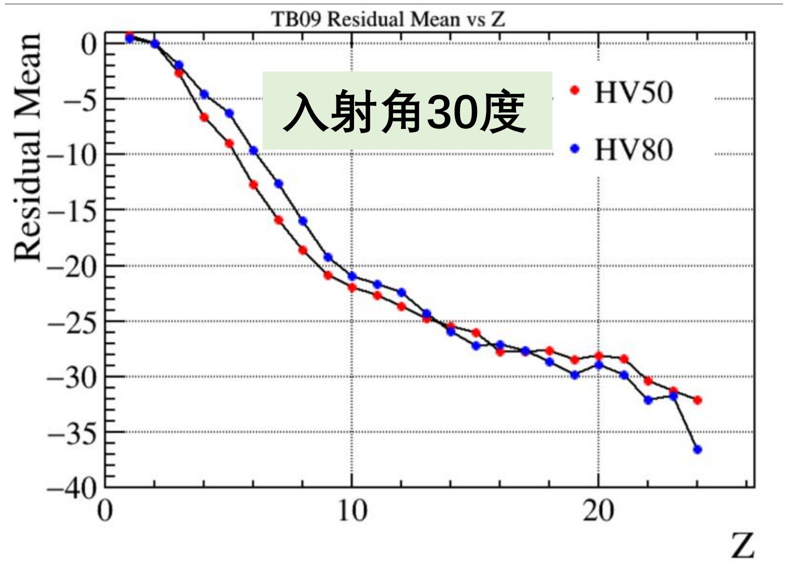

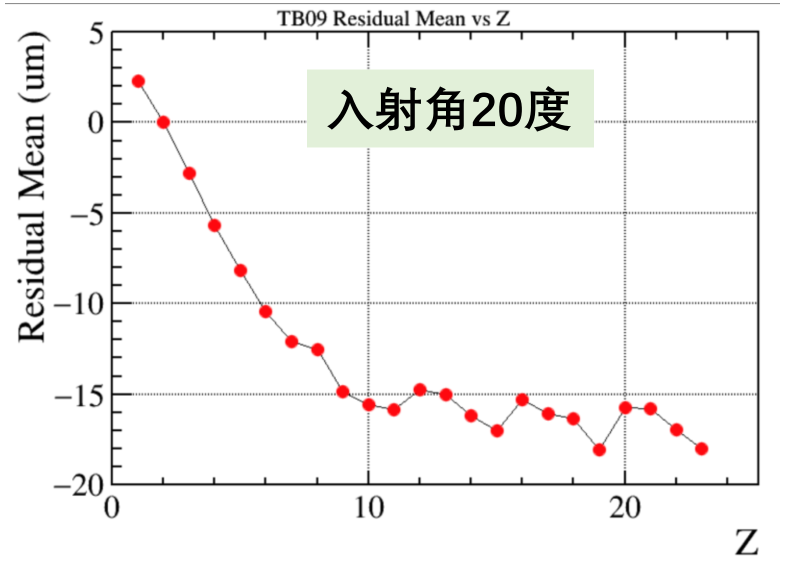

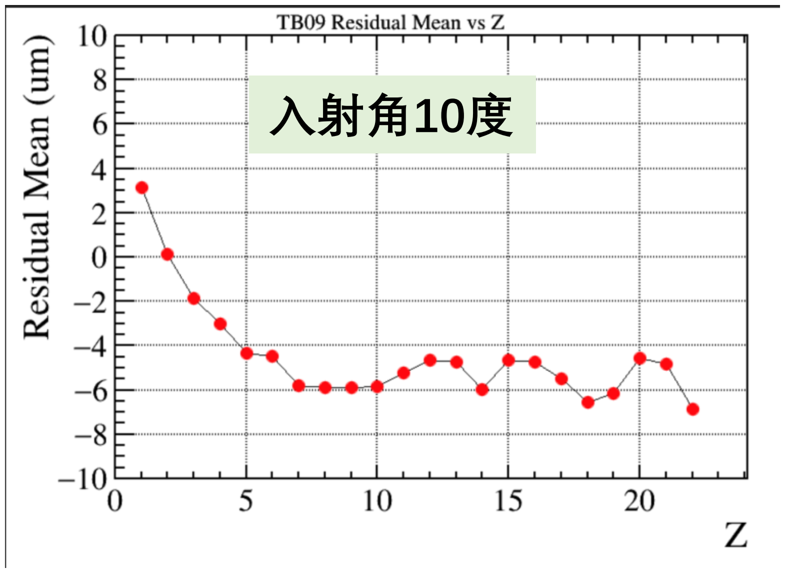

- The shift value increases with the incident angle, which is consistent with the AMS-02 results
- No obvious changes with HV were observed
- Simulation work in progress (work with junior students)

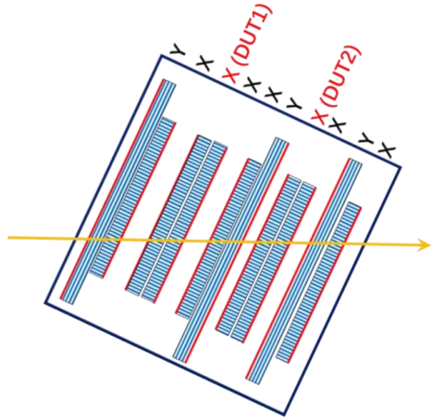

Challenges in implementation

- Different incident ions lead to huge signal variations (ranging from single digits to tens of thousands)
- Inputs spanning multiple orders of magnitude pose a challenge for neural networks (**Instability**)
  - Conventional normalization (Min–Max, Gaussian) distorts cluster structures and degrades precision

Our solution: digital vector encoding

- Expand values into decimal digit sequences, with each digit ∈ [0,9]
- Use fixed-length vectors (6 significant digits with one decimal place) as neural network inputs
- **Example:**

value: 13854 → [1, 3, 8, 5, 4,0]

Cluster: raw cluster [438.4, 2313.4, 9408.4, 5121.1, 768.2]

↓ ↓ ↓ ↓ ↓

Encoding cluster [[0,0,4,3,8,4], [0,2,3,1,3,4], [0,9,4,0,8,4], [0,5,1,2,1,1], [0,0,7,6,8,2]]

精确控制潜空间形状：PDF Loss

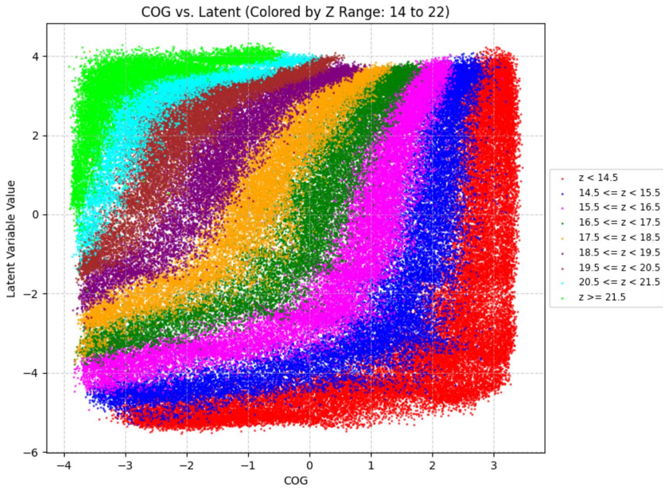

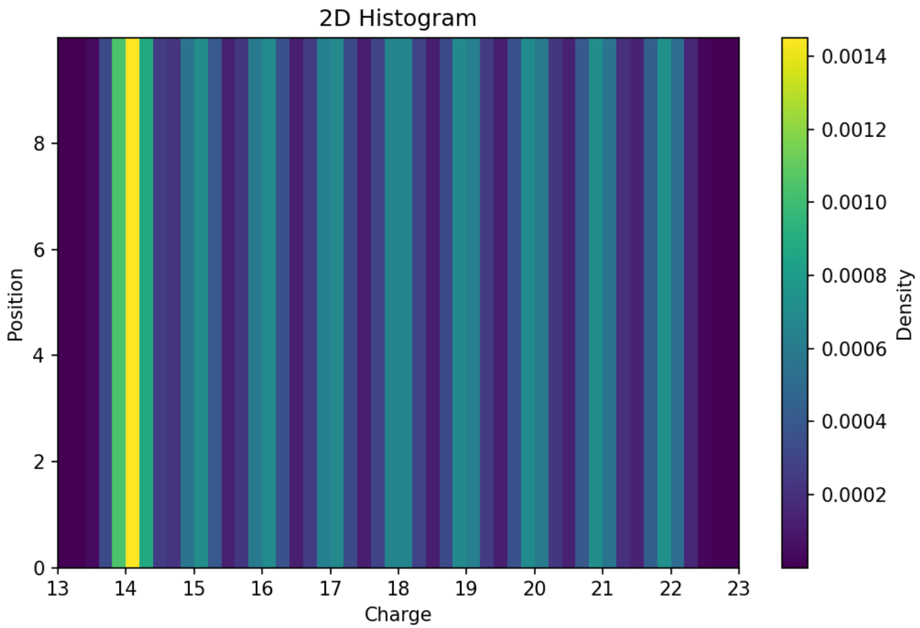

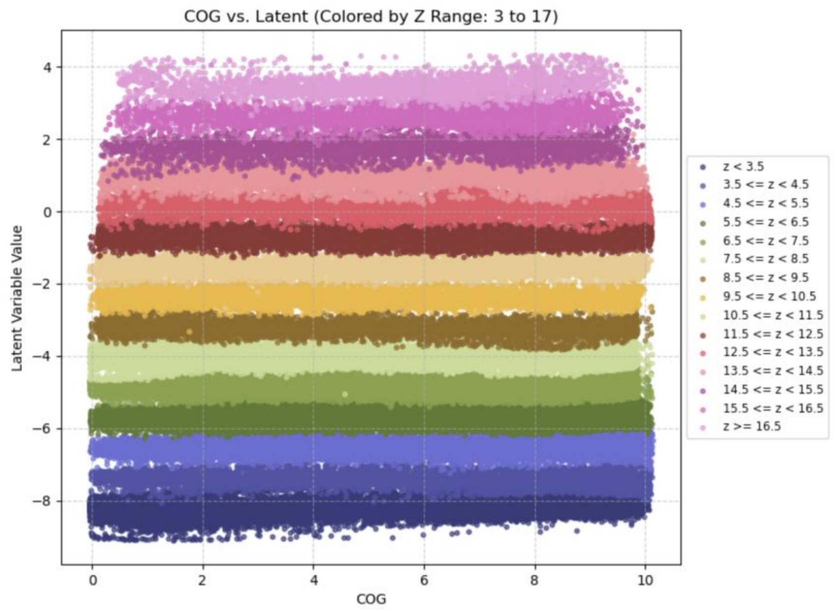

- 粒子电荷与相对击中位置应当是独立的，并且各自满足分布：
  - 相对击中位置：均匀分布 $U(x)$
  - 粒子电荷： Gaussian mixture distribution $\mathrm{GMM}(z)$
- 因此可以给出潜空间的目标分布：

$$f(x,z)=U(x)\cdot \mathrm{GMM}(z)$$